T.R.
GEBZE TECHNICAL UNIVERSITY
INSTITUTE OF BIOTECHNOLOGY

INVESTIGATION OF ANTI-CANCER EFFECTS OF *CISTUS CRETICUS L.* (CRETAN ROCKROSE) GROWN UNDER DIFFERENT SALT STRESS LEVELS IN PANCREATIC CANCER CELL LINES

BURÇİN ÖZBEKLE
A THESIS SUBMITTED FOR THE DEGREE OF
MASTER OF SCIENCE
INSTITUTE OF BIOTECHNOLOGY

GEBZE
2023

T.R.

GEBZE TECHNICAL UNIVERSITY

INSTITUTE OF BIOTECHNOLOGY

INVESTIGATION OF ANTI-CANCER EFFECTS OF *CISTUS CRETICUS L.* (CRETAN ROCKROSE) GROWN UNDER DIFFERENT SALT STRESS LEVELS IN PANCREATIC CANCER CELL LINES

BURÇİN ÖZBEKLE

A THESIS SUBMITTED FOR THE DEGREE OF MASTER OF SCIENCE

INSTITUTE OF BIOTECHNOLOGY

THESIS SUPERVISOR

PROF. DR. ELİF DAMLA ARISAN

THESIS CO-SUPERVISOR

Asst. Prof. BAHAR YILDIZ KUTMAN

GEBZE

2023

T.R.
GEBZE TEKNİK ÜNİVERSİTESİ
BİYOTEKNOLOJİ ENSTİTÜSÜ

PANKREAS KANSERİ HÜCRE HATLARINDA FARKLI TUZ STRESİ SEVİYELERİ ALTINDA YETİŞTİRİLEN *CISTUS CRETICUS L.*'NİN (GİRİT LADENİ) ANTİ-KANSER ETKİLERİNİN ARAŞTIRILMASI

BURÇİN ÖZBEKLE
YÜKSEK LİSANS TEZİ
BİYOTEKNOLOJİ ENSTİTÜSÜ

TEZ DANIŞMANI
PROF. DR. ELİF DAMLA ARISAN

TEZ EŞ DANIŞMANI
Dr. Öğr. Üyesi BAHAR YILDIZ KUTMAN

GEBZE
2023

GEBZE TEKNİK ÜNİVERSİTESİ	**YÜKSEK LİSANS JÜRİ ONAY FORMU**

GTÜ Biyoteknoloji Enstitüsü Yönetim Kurulu'nun …..…/…..…/..…… tarih ve ..……/……..… sayılı kararıyla oluşturulan jüri tarafından …..…/…..…/..…… tarihinde tez savunma sınavı yapılan Burçin Özbekle'nin tez çalışması Biyoteknoloji Anabilim Dalında YÜKSEK LİSANS tezi olarak kabul edilmiştir.

JÜRİ

ÜYE
(TEZ DANIŞMANI) : Prof. Dr. Elif Damla ARISAN

ÜYE : Prof. Dr. Pınar OBAKAN YERLİKAYA

ÜYE : Dr. Öğr. Üyesi Mehmet ÖZBİL

ONAY

Gebze Teknik Üniversitesi Biyoteknoloji Enstitüsü Yönetim Kurulu'nun

..…/……/…… tarih ve ……/…..... sayılı kararı.

İMZA/MÜHÜR

SUMMARY

Pancreatic cancer is the seventh leading cause of cancer-related deaths worldwide, with high mortality rates. Over 90% of individuals with pancreatic cancer have oncogenic KRAS mutations, whereas the suppressor genes SMAD4, TP53, and CDKN2A have inactivating mutations. *Cistus creticus* L. subsp. is a characteristic species commonly distributed in the Mediterranean region. It has been proved to *C. creticus* extracts show antibacterial, anti-inflammatory, and anti-cancer traits. In this study, *C. creticus* plants which were grown in hydroponic culture under different salinity levels (0, 30 and 60 mM NaCl) were extracted using two solvents (70% ethanol and distilled water). The effect of salinity stress in plant extracts, bioactive compound content and therapeutic impact on cell death and cell survival in pancreatic cancer cell lines were studied. Pancreatic cancer cell lines (PANC-1, MIA PaCa-2, and AsPC-1) were treated with different concentrations of *C. creticus* extracts and cell survival, lipid metabolism, autophagy, apoptosis, and necrosis signaling pathways were studied. Especially, ethanol extraction of *C. creticus* showed a remarkably therapeutic effect on cell death and cell survival through reduced Reactive Oxygen Species (ROS) and reduced cellular mitochondrial activity with the increasing doses. Ethanol extracts of *C. creticus* have higher polyphenolic content and are more effective than water extracts. It has been found that *C. creticus* is an important lipid metabolism-targeted antioxidant in pancreatic cancer cell lines. This research could be important to evaluate how abiotic stress on *C. creticus* relates to the therapeutic effectiveness of *C. creticus* on cancer.

Key Words: Pancreatic Cancer, *Cistus creticus*, Cell Death, Autophagy, Lipid Metabolism.

ÖZET

Pankreas kanseri, yüksek ölüm oranlarıyla dünya çapında kansere bağlı ölümlerin yedinci önde gelen nedenidir. Pankreas kanseri olan bireylerin %90'ından fazlasında onkojenik KRAS mutasyonları bulunurken, baskılayıcı genler olan SMAD4, TP53 ve CDKN2A inaktive edici mutasyonlarına da sahiptir. *Cistus creticus* L. subsp., genellikle Akdeniz bölgesinde yaygın olarak yayılım gösteren karakteristik bir türdür. *C. creticus* ekstraktlarının antibakteriyel, anti-inflamatuar ve anti-kanser özellikleri gösterdiği kanıtlanmıştır. Bu tez çalışmasında, farklı tuzluluk seviyelerinde (0, 30 ve 60 mM NaCl) hidroponik kültürde yetiştirilen *C. creticus* bitkileri, iki çözücü (%70 etanol ve distile su) kullanılarak ekstrakte edilmiştir. Pankreas kanseri hücre hatlarında bitki ekstraktlarındaki tuzluluk stresinin etkisi, biyoaktif bileşik içeriği ve terapötik etkinin hücre ölümü ve hücre sağkalımına etkisi incelenmiştir. Pankreas kanseri hücre hatları (PANC-1, MIA PaCa-2 ve AsPC-1) farklı *C. creticus* konsantrasyonları ile tedavi edilmiştir ve hücre sağkalımı, lipid metabolizması, otofaji, apoptoz ve nekroz sinyal yolları incelenmiş. Özellikle *C. creticus*'un etanol ekstraksiyonu, artan dozlarla birlikte azalan Reaktif Oksijen Türleri (ROS) ve azalan hücresel mitokondriyal aktivite ile hücre ölümü ve hücre sağkalımı üzerinde dikkate değer bir terapötik etki göstermiştir. *C. creticus*'un etanol özleri daha yüksek polifenolik içeriğe sahiptir ve su özlerinden daha etkilidir. *C. creticus*'un pankreas kanseri hücre hatlarında lipit metabolizması hedefli önemli bir antioksidan olduğu bulunmuştur. Bu araştırma, *C. creticus* üzerindeki abiyotik stresin *C. creticus*'un kanser üzerindeki terapötik etkinliği ile nasıl ilişkili olduğunu değerlendirmek için önemli olabilir.

Anahtar Kelimeler: Pankreas Kanseri, *Cistus creticus*, Hücre Ölümü, Otofaji, Lipit Metabolizması.

ACKNOWLEDGEMENTS

I would like to express my deep and sincere gratitude to my supervisor Prof. Dr. Elif Damla ARISAN, who contributes in shaping my overall personal and professional growth in academia. Her belief in my abilities and her motivating words have been a constant source of inspiration, especially during challenging times. Her guidance and mentorship have helped me navigate through obstacles, and her constructive criticism has pushed me to strive for excellence in my work. Her mentorship has extended beyond the boundaries of academia, as she has generously shared her wisdom, insights, and experiences, imparting invaluable life lessons that will undoubtedly resonate with me for years to come.

I also would like to express my gratitude and sincere thanks to my co-supervisor Asst. Prof. Bahar YILDIZ KUTMAN for her valuable collaborations and structure of my thesis. I am thankful for her invaluable contributions and unwavering support throughout the completion of my master's thesis.

I want to thank Yağmur ARIKAN for her contribution to my thesis study.

I want to thank my dear friend Ayyüce SEVER for sharing her experiences from the very beginning of our lab journey together. Her presence in the lab has made the research process more enjoyable, meaningful, and fulfilling.

I want to thank Gizem KUGU for her unwavering love, support, and understanding throughout the completion of my master's degree. Her presence has been a source of strength, inspiration, and unwavering support. I am grateful for her belief in me, intellectual contributions, and the profound impact she has had on both my academic and personal growth.

I would like to express my heartfelt gratitude and thanks to my beloved mother Gülgün ÖZBEKLE and my lovely sister Buket ÖZBEKLE for their unwavering support and encouragement throughout the completion of my master's degree.

I would like to dedicate my master's thesis in the loving memory of my dear father Mustafa Çetin ÖZBEKLE who has been the driving force behind my academic journey.

Finally, this study was funded by The Scientific and Technological Research Council of Turkey (TUBITAK) with the Project Number of 122Z186. We would like to thank TUBITAK for providing funds within the scope of this project.

TABLE OF CONTENTS

LIST of ABBREVIATIONS and ACRONYMS

Abbreviations and Acronyms		**Explanations**
α	:	Alpha
β	:	Beta
µ	:	Micro
h	:	Hour
µg	:	Microgram
µl	:	Microliter
µm	:	Micrometer
ml	:	Milliliter
mM	:	Millimolar
nm	:	Nanometer
kDa	:	Kilodaltons
x g	:	Times gravity
%	:	Percentage
°C	:	Degree Celsius
ACC	:	Acetyl-CoA Carboxylase
AceCS1	:	Acetyl Coenzyme A Synthetase 1
AMPK	:	AMP-Activated Protein Kinase
ATG12	:	Autophagy Related 12
ATG16L1	:	Autophagy Related 16 Like 1
ATG5	:	Autophagy Related 5
ATG7	:	Autophagy Related 7
ATP	:	Adenosine Triphosphate
BODIPY	:	Fluorinated Boron-Dipyrromethene
DAPI	:	4′,6-diamidino-2-phenylindole
dH_2O	:	Distilled water
DiOC6	:	3,3′-dihexyloxacarbocyanine iodide
DMEM	:	Dulbecco's Modified Eagle Medium
DMSO	:	Dimethyl sulfoxide
DNA	:	Deoxyribonucleic Acid

EDTA	:	Ethylenediamine tetra acetic acid
EtOH	:	Ethanol
FASN	:	Fatty Acid Synthase
LAMTOR1	:	Late endosomal/lysosomal adaptor, MAPK and MTOR activator 1
LC3A/B	:	Microtubule-associated protein 1A/1B-light chain 3
MLKL	:	Mixed Lineage Kinase Domain Like Pseudokinase
MTOR	:	Mammalian Target of Rapamycin
NaCl	:	Sodium Chloride
PARP	:	poly (ADP-ribose) polymerase
PBS	:	Phosphate Buffered Saline
PI	:	Propidium Iodide
RAGC	:	Ras-related GTP Binding C
RAS	:	Rat Sarcoma
RIP	:	Ribosome-Inactivating Protein
ROS	:	Reactive Oxygen Species
RPMI-1640	:	Roswell Park Memorial Institute
TBS	:	Tris-Buffered Saline
TBS-T	:	Tris-Buffered Saline-Tween 20

LIST OF FIGURES

LIST OF TABLES

1. INTRODUCTION

1.1. Pancreatic Cancer

The pancreas is a 15-cm long, tube-shaped organ which is placed in the upper abdomen between spine and stomach. Noncancerous, normal pancreas cells consist of five groups: acinar cells secrete digestive enzymes; ductal secretes bicarbonate; endocrine islet cells secrete hormone; stellate cells that are inactive and centroacinar cells are located the translational region between acinar and ductal cells (Figure 1.1.) [1]. On the other hand, when pancreas undergoes abnormal DNA mutations, pancreatic cells to grow uncontrollably and divide and form tumors. Pancreatic cancer is one of the most lethal and aggressive cancer type and it manifests at an advanced stage that has frequently spread to other body parts by the time it is diagnosed. In pathologically, pancreatic cancer is general term for malignant tumors that formed in epithelial cells of glandular parts in pancreatic ductal cells which is called adenocarcinoma. More than 90% of pancreatic cancers result from pancreatic ductal adenocarcinoma (PDAC) [2].

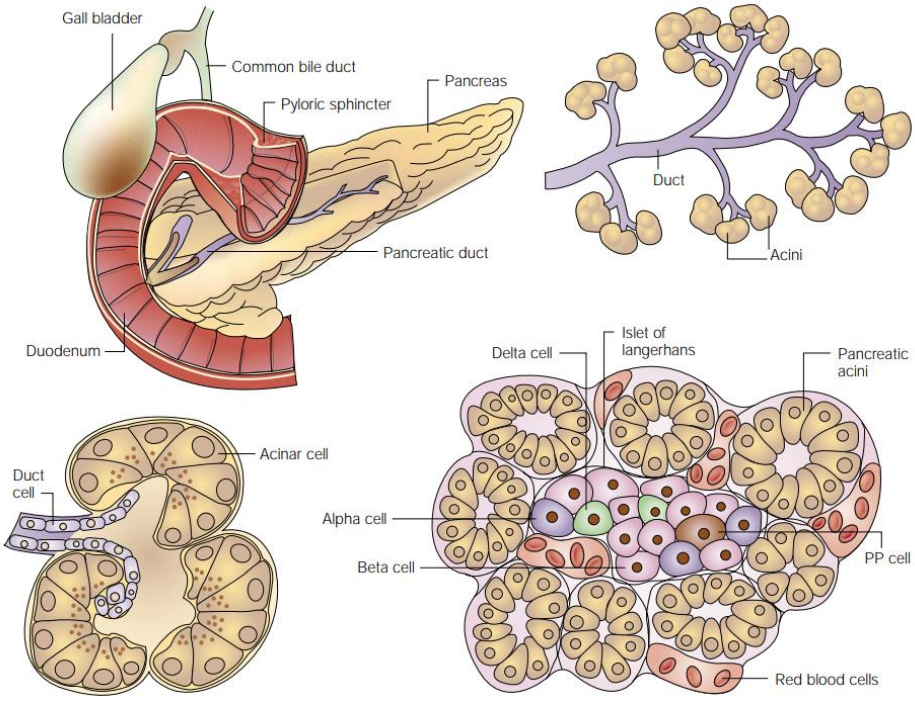

Figure 1.1. The anatomy of the pancreas.

1.1.1. Epidemiology of Pancreatic Cancer

Pancreatic cancer is the seventh greatest cause of cancer-related deaths globally which has high mortality rates. According to GLOBOCAN 2020 estimation, there are 466,000 deaths among 496,000 new cases. Pancreatic cancer has a 5-year survival rate which is the lowest (9%) of other cancer types. If patients undergo resection surgery, the 5-year survival rate for any stage patients is 31% [3]. According to Global Cancer Observatory by World Health Organization, age standardized rates in 2020 for both sexes and all ages in pancreatic cancer and mortality rate worldwide between 2015-2018 is shown in Figure 1.2. [4].

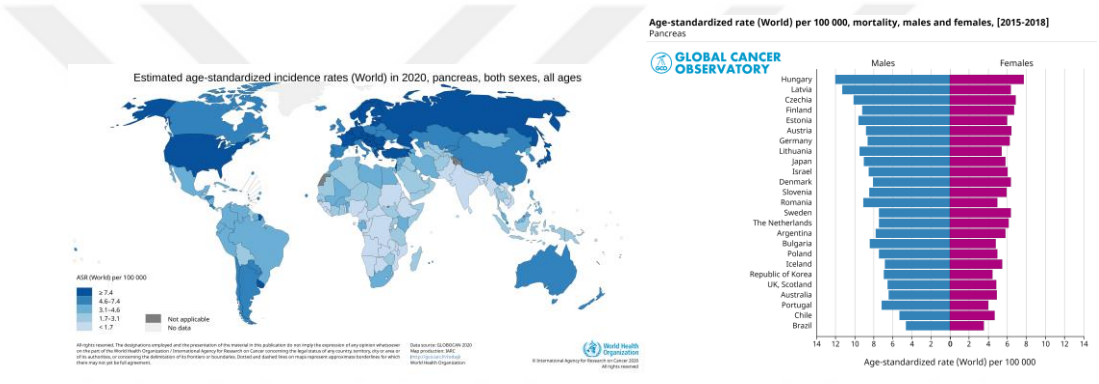

Figure 1.2. The age standardized rates in 2020 for both sexes and all ages in pancreatic cancer and mortality rate in world between 2015-2018, respectively by International Agency for Research on Cancer.

1.1.2. Risk Factors in Pancreatic Cancer

Risk factors for pancreatic cancer can be classified as two groups: non-modifiable and modifiable. Non-modifiable risk factors are age, gender, ethnicity, blood group, genetic susceptibility, and family history whereas modifiable risk factors include intestinal microflora, alcohol, smoking, obesity, dietary and infection.

In non-modifiable risk factors, most of the new cases and death by pancreatic cancer occur in patients which are over 55 years old. The highest percentage of death occurs at the age of 72-80 years. The incidence and death rate of pancreatic cancer is higher in men than women globally. The increased risk of pancreatic cancer is common in African Americans than Caucasians whereas the risk is lowest in Asian and Pacific Islanders. Patients with O blood have lower risk than patients with blood

type A, B and AB to risk in developing pancreatic cancer due to alterations in glycosyltransferase and inflammatory states among blood groups [5]. The gut microbiota also has an important role in pancreatic cancer. Higher levels of *Granulicatella adiacens* and *Porphyromonas gingivalis* microorganisms and lower levels of *Streptococcus mitis* and Neisseria elongate are linked in increased pancreatic cancer incidence [6]. In addition, patients who have two or more-degree relatives that were diagnosed with pancreatic cancer have nine times higher risk to have the same disease. 80% of pancreatic cancer results from sporadic mutations followed by point mutations which can be commonly developed in K-RAS, TP53, SMAD4, CDKN2A, BRCA2, MMR genes [7].

In modifiable risk factors, smokers have a 74% higher chance of developing pancreatic cancer. High alcohol consumption also increases the risk of pancreatic cancer by 15% which can also cause pancreatitis. According to epidemiological data, obesity is another important risk factor associated with KRAS mutation and type 2 diabetes that interferes with the downstream signals for pancreatic cancer [8].

1.1.3. Treatment Models in Pancreatic Cancer

Radiotherapy, chemotherapy, surgery, targeted therapy, and palliative care are the general treatment modalities for pancreatic cancer as well as immunotherapy, targeted therapy and microbial therapy. Treatment models can be dependent on the stage of the cancer [9].

Depending on the anatomical location of tumor in pancreas, surgical resections include pancreaticoduodenectomy (Whipple's procedure), distal or total pancreatectomy. Pancreatic cancer patients who have been impacted by artery are generally not considered suitable for resection [10]. However, pancreatic cancer patients can undergo tumor resection after neoadjuvant chemotherapy which results in a significantly longer survival period.

Median survival for pancreatic cancer is up to 10-12 months with treatment whereas 5-6 months without treatments due to the dismal diagnosis at advanced stage which very small number of the pancreatic cancer patients are the candidates for surgical resection [11].

Adjuvant chemotherapy is commonly used after curative surgical resection. The most common standard of care in first-line chemotherapies which are currently used: FOLFIRONOX, oxaliplatin or gemcitabine added with albumin-bound paclitaxel [12].

As an alternative approach, neoadjuvant therapy which is used prior to surgery provides better tumor control and survival with increased life quality. Potential metastatic tumors can be eliminated by pre-operative treatment. Local tumors can be easily removed by neoadjuvant chemotherapy [13].

Radiation is another therapy that is used to destroy cancer cells by X-Rays, preventing them from proliferating on patients with advanced pancreatic cancer. X-rays, gamma rays, heavy particles and electron are used in external beam radiation therapy which requires multiple repeats of treatment whereas brachytherapy is used as internal radiotherapy in pancreas by laparoscopy or surgery in the adjacent tissue to pancreas [14].

Due to genetic alterations lead to PDAC, targeted therapies to specific genes are promising to develop new drugs and their combinations. 10-15% of PDAC patients have inherited mutations as well as all the pancreatic cancer patients have somatic mutations in driver genes [11].

New studies on the tumor and microenvironment alteration affect metastasis, progression and development of pancreatic cancer that aims to understand targetable pathways on molecular basis. It is important that combined therapy should be created to apply personalized medicine based on specific genes to interfere cellular processes, pathways and transcriptional activation of gene which results in cancer.

BRCA1/BRCA2 mutations: The most studied mutations are BRCA1 (breast cancer type 1 susceptibility protein) and BRCA2 genes which are responsible in double-strand DNA breaks repairing by germline homologous DNA repair (HDR) mechanism. They are mainly indicators for breast and ovarian cancer as well as pancreatic cancer that can be found in 5-10% of cases of PDAC patients. Niraparib and Olaparib which are PARP inhibitors can also be potential treatment for BRCA mutations. Repair of single-strand breaks are blocked which is leading to double-strand breaks. However, they cannot be repaired by tumors that deficient HDR result in apoptosis and cell cycle arrest [15].

KRAS mutations: KRAS (Kirsten rat sarcoma viral oncogene homolog) mutations are identified in 90-95% of PDAC patients and may be the one of the important driving forces for pancreatic carcinogenesis. KRAS is a membrane bound GTPase which is a part of the cellular growth via MAPK and PI3K pathways when it is in GTP form. The KRAS mutations reduce KRAS intrinsic GTPase activity and prevent GTPase-activating proteins (GAPs) from changing from the active GTP-bound form to the inactive GDP-bound form [16]. Sotorasib and Adagrasib are now being used clinically as KRAS inhibitors [17].

ARID1A mutations: ARID1A (AT-rich interaction domain 1A) is another frequently mutated gene which is a poor prognostic predictor as well as have the ability of tumor suppressing and oncogenic properties associated in several cellular processes such as DNA damage repair, transcriptional control, and telomere maintenance [18]. Clinical studies showed that ARID1A mutated tumors are sensitive to PARP inhibitors [19].

1.2. Molecular Metabolism in the Formation of Pancreatic Cancer

Pancreatic cancer cells have oncogenic KRAS mutations that occur in over 90% of patients and inactivating mutations that are found in suppressor genes which are SMAD4, TP53 and CDKN2A. The tumor suppressor gene TP53 has inactivating mutations in 50–74% of cases of pancreatic cancer. Cancer cells are able to avoid cell cycle checkpoints and apoptotic signals when TP53 is inactivated because it inhibits the ability to recognize DNA damage and prevents cell cycle arrest. Approximately 46–60% of pancreatic cancer tumors have CDKN2A mutations, which can result in disruption of the cell cycle and subsequent carcinogenesis by causing the loss of control of the cyclin-dependent kinase (CDK) 4 and CDK6 cell cycle checkpoints. On the other hand, SMAD4 mutation which may arise in the last stages of pancreatic cancer is present in between 31-38% of pancreatic tumors [20].

Reprogrammed cellular energy metabolism is one the most important hallmarks of cancer which affects the survival, division, and unlimited cell control of tumor cells through numerous metabolic interactions with both adjacent normal cells and extracellular matrix (ECM) inside the tumor microenvironment. These metabolic

interactions can also influence epigenetic regulation to increase pancreatic metastasis and tumorigenesis [21].

Moreover, cancer cells show tremendous growth advantageous within relatively nutrient-poor and hypoxic environments. The survival mechanism of cancer cells is based on three ways: improving nutrient uptake through recycling and scavenging, updating the usage of nutrients such as glucose, lipids and amino acids and conducting metabolic interaction in between tumor microenvironment [22].

1.2.1. Glucose and Amino Acid Metabolism

It was first demonstrated that tumor cells use more glucose than normal cells to convert carbon from glucose to lactate even in the presence of enough oxygen. This effect in cancer cells is the Warburg effect which is also called aerobic glycolysis [23]. Tumor cells also need rapid and extensive biosynthesis with several intermediates to arrange the ATP/ADP ratio. It is also crucial for preserving redox balance and chromatin state regulation. This feature provides pancreatic cancer cells to generate an environment with inadequate immunity and encourages cancer cells to invade [24]. It is also shown that cancers with various tissue origins display distinctive metabolic alterations even when they are influenced by the same oncogenes [25]. In glucose metabolism, overexpression of the glucose transporter (GLUT1) and other glycolytic enzymes such as hexokinase 1-2, phosphofructokinase-1 and lactate dehydrogenase increase the glucose absorption and upregulate glycolysis by oncogenic KRAS. In addition, limited oxidative phosphorylation (OXPHOS) and phosphorylated pyruvate dehydrogenase kinase-1 are produced in pancreatic cancer cells as a result of mutant KRAS signaling that encourages mitochondrial translocation of phosphoglycerate kinase-1. The hexosamine biosynthesis pathway (HBP) and the nonoxidative branch of the pentose phosphate pathway (PPP) are the anabolic pathways that are biosynthesized precursors by oncogenic KRAS-induced enhanced glycolysis [26].

TP53 is also another important metabolic reprogramming gene in pancreatic cancer cells. P53 and KRAS are able to encourage metabolic alterations even in absence of malignant transformation event. Mutant TP53 has the ability to enhance glycolysis in pancreatic cancer cells by increasing paraoxonase-2 expression and

inhibiting the expression of TP53-induced glycolysis regulatory phosphatase [27]. Moreover, TP53 gains new functions by improving the Warburg effect in order to increase GLUT1 translocation to the plasma membrane of the cell and TP53 mutations also can lower mitochondrial activity to inhibit progression of pancreatic cancer [28].

Amino acid metabolism is also extremely important for the development of pancreatic cancer. Glutamine (Gln) is the most abundant amino acid to supply carbon and nitrogen to cancer cells in the bloodstream. Gln is required for pancreatic cancer growth by redox homeostasis in a metabolic pathway that is activated by KRAS. Moreover, glutamate (Glu) is deaminated by glutaminase 1 (GLS1) with help of Gln entry into mitochondria. As a result, glutamate dehydrogenase (GDH) is suppressed while the cytoplasmic aspartate transaminase (GOT1) is upregulated in order to pyruvate formation [29]. Therefore, redox control in pancreatic cancer cells and resistance to reactive oxygen species (ROS) is developed with enough reducing power which leads to an acidic microenvironment. However, cancer cells can overcome increased ROS production and promote survival by upregulating the GOT1 expression. So that, tumor growth can be reduced when components of downstream glutamine metabolism are inhibited [30]. In addition, upregulation of arginase 2 that converts arginine into urea or ornithine in mitochondria occurred in response to obesity and active protein kinase AKT which speed up the growth of cancer [31]. The overall relationship of metabolic pathway in pancreatic cancer is shown in Figure 1.3. [32].

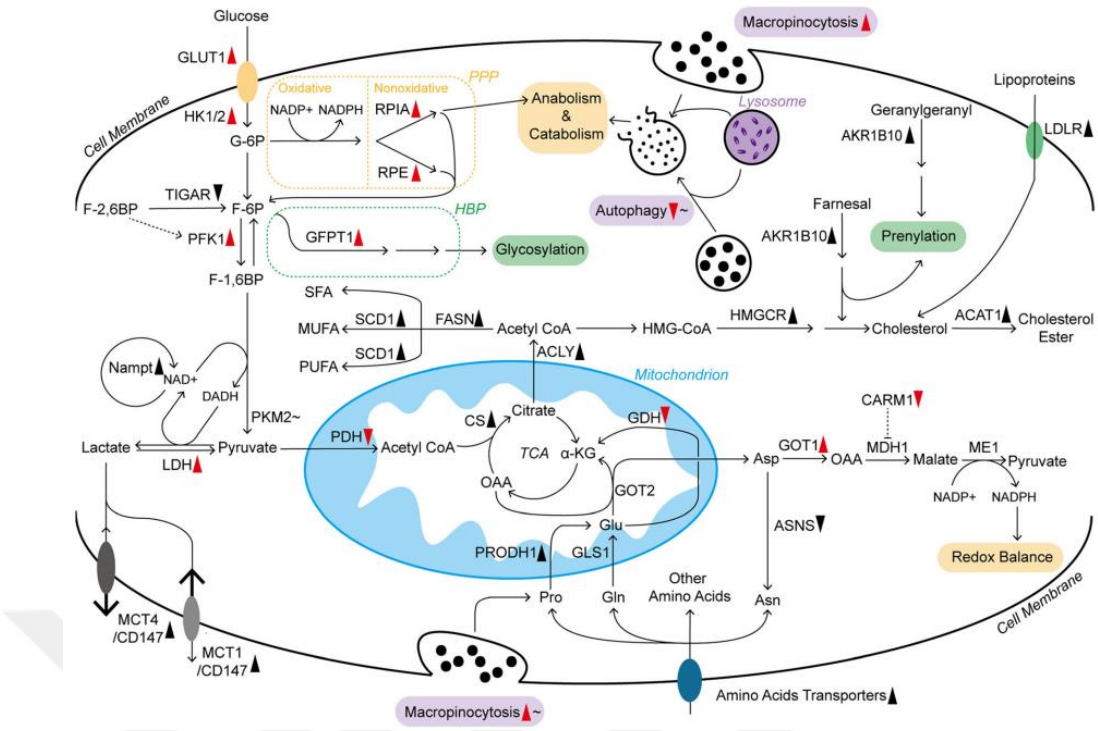

Figure 1.3. Metabolic pathway organization in pancreatic cancer cells.

1.2.2. Fatty Acid and Lipid Metabolism

Lipid metabolism in pancreatic cancer is essential for its progression where the dysregulation in metabolism and the conversion of nutrients into metabolic intermediates for the cellular structure, signaling molecule production and energy storage occurs. Lipid metabolism is also generating substrate and other signaling molecules for protein posttranscriptional modification as well as building blocks for rapid membrane assembly. Approximately 93% of triacylglycerol fatty acids in tumor cells are de novo produced from mitochondrial citrate which is also the intermediate between mitochondria and cytosolic acetyl coenzyme A (CoA). Other important enzymes in lipid metabolism that upregulated in pancreatic cancer are fatty acid synthase (FASN), ATP citrate lyase (ACLY) and citrate synthase (CS). In addition, extracellular lysophospholipid-derived monounsaturated fatty acid absorption from hypoxia or oncogenic KRAS could also be induced [33].

Pyruvate that is produced by glycolysis is transported to mitochondria where it is converted into acetyl-CoA pyruvate dehydrogenase. Then citrate formation occurs by highly active citrate synthase from mitochondrial acetyl-CoA. Then, citrate carrier subsequently transports citrate from the mitochondria to the cytosol where it is

transformed into acetyl-CoA by ATP-Citrate lyase (ACLY). Then, acetyl-CoA is converted to malonyl-CoA by Acetyl-CoA (ACC) followed by the coupling of acetyl-CoA and malonyl-CoA to fatty acid synthase (FASN) which provides acetyl-group condensation for saturated palmitic acid generation [34].

In general, the expression of ACLY is noticeably higher in pancreatic cancer cells and PI3K/Akt signaling pathway controls de novo lipid synthesis in response to glucose. ACLY knockdown can inhibit this process as well as reduce cancer cell proliferation. Considering overexpressed ACC in cancer cells, the inhibition of ACC can reduce fatty acid production and tumor growth which is formed by oncogenic KRAS with Trp53 or Stk11-knockouts. Serine/threonine kinase 11 (STK11) is also called liver kinase B1 (LKB1) which activates AMP-activated protein kinase (AMPK) which leads to ACC inhibition and phosphorylation by AMPK. In pancreatic cancer cells, activation of EGFR signaling results in the overexpression of FASN in an ERK-dependent manner. In addition, the transcription factor sterol regulatory element-binding protein 1c (SREBP1c), which is downstream of various signaling pathways and factors such the PI3K/Akt and MEK/ERK pathways controls the expression of FASN [35].

1.2.3. mTOR Signaling Pathway

The mammalian target of rapamycin (mTOR) is a serine/threonine protein kinase which is a primary catalytic subunit of the two multiprotein mTOR complex 1 (mTORC1) and mTOR complex 2 (MTORC2) and the signaling of these complexes is closely linked with PI3K activation (Figure 1.4.). The main differences between these two complexes are mTORC1 couples with Raptor which is a regulatory protein associated with mTOR and mTORC2 couples with Rictor which is a rapamycin-insensitive companion of mTOR [36].

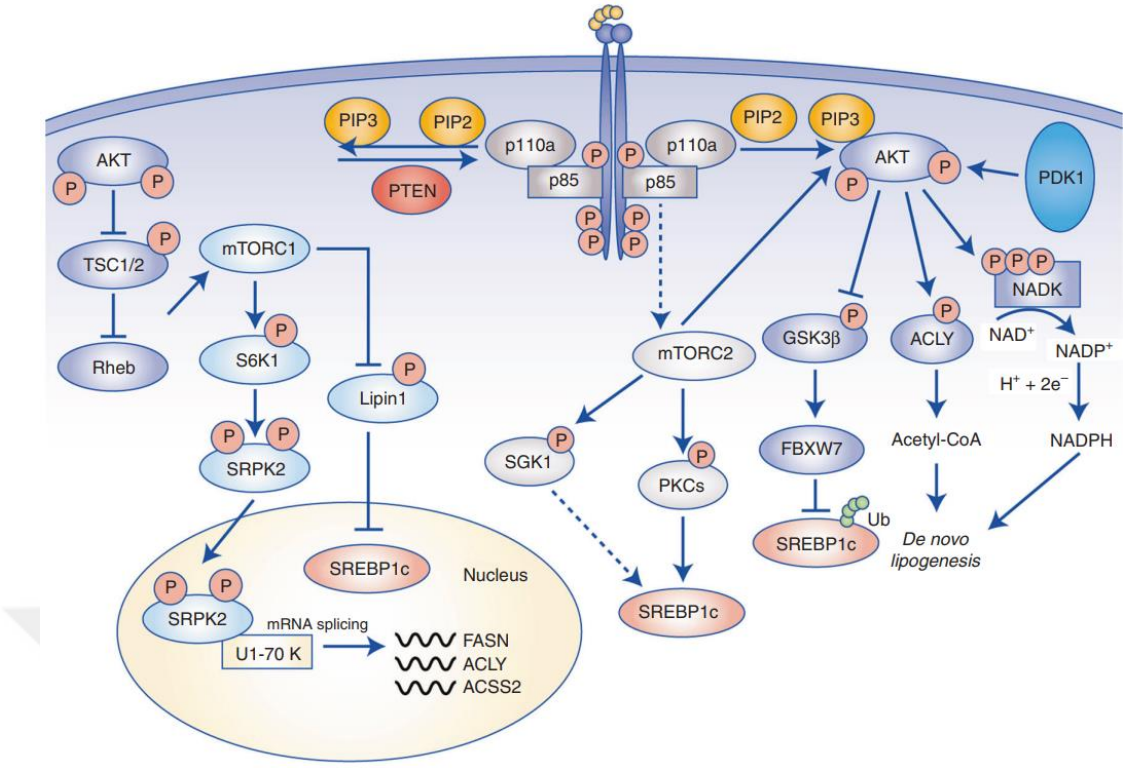

Figure 1.4. The PI3K-mTOR signaling pathway modulates lipid metabolism.

AKT is responsible in activation of MTORC1 by phosphorylation and inactivation of Tuberous sclerosis complex components 1 and 2 (TSC1/2). SREBP1c's migration from the ER membrane to the Golgi apparatus is upregulated by AKT where it can be converted into the transcriptionally active form. mTORC1 prevents membrane-derived cholesterol from reaching lysosomes and subsequent ER localization, which results in activation of SREBP2. In addition, SREBP1 which is transcriptional regulator in lipogenesis is activated by PI3K–AKT–mTORC1-dependent mechanisms whereas lipogenic enzymes such as FASN, ACC1 and ACLY are inhibited by MTORC1 inhibition through raptor or rapamycin knockouts [37]. Additionally, Lipin-1 is inactivated and phosphorylated by mTORC1 which result in sequestration to cytoplasm as well as lipin-1 translocate to the nucleus in response to mTORC1 inhibition, which results in considerable nuclear remodeling and decreased SREBP transcriptional activity [38]. The PI3K-mTOR signaling pathway which is modulated by lipid metabolism is shown in Figure 1.4. [39].

1.2.4. AMPK Signaling Pathway

AMP-activated protein kinase (AMPK) is a widely recognized energy sensor within cells and its activation depends on various signals and metabolic pathways in response to aging, obesity, calorie restriction and exercise. It is also demonstrated that, LKB1 which is an upstream kinase to activate AMPK shows tumor suppressive activity. The main principle of AMPK is maintaining energy homeostasis and acting like a metabolic gatekeeper for cells. Increased AMP/ATP or ADP/ATP levels are recognized and sensed by AMPK and its activation is promoted by LKB1 and calcium/calmodulin-dependent protein kinase 2 (CaMKK2 or CaMKKβ). As a result, AMPK upregulate catabolic processes such as TCA cycle, glycolysis, and fatty acid oxidation to produce energy for cells whereas it inhibits fatty acid synthesis and protein synthesis in order to limit the energy consumption by inactivating mTORC1[40].

Stability and enzymatic activity of AMPK are influenced by post-translational modifications of AMPK such as phosphorylation of AMPK from Threonine 172 (T172) residue which highly increase the AMPK activity. Phosphorylation is an important biological process for mitochondrial dynamics, cellular metabolism, transcription of genes, cell cycle progression and assembly of Golgi. Additionally, the AMPK phosphorylation of ACC results in the suppression of lipogenesis. Mitophagy is induced by phosphorylation of ULK1 (unc-51 like autophagy activating kinase 1) and mitochondrial fission is induced by the phosphorylation of MFF (mitochondrial fission factor) via AMPK [41].

AMPK modulating medications have been used both in in vivo and in vitro studies to analyze the function of AMPK in cancer progression and initiation. AMPK can act as a suppresser or promoter for cancer which depends on biological circumstances. In de novo fatty acid synthesis, active AMPK can phosphorylate and inhibit ACC and SREBP1c. In addition, RAPTOR can also be phosphorylated by AMPK results in mTORC1 inhibition, metabolic stress, and apoptosis. Cell cycle arrest is induced by AMPK via p53, retinoblastoma protein (pRb) and p27 activation which are important tumor suppressors [42].

It is essential for cancer cells to be able to overcome metabolic stresses such as hypoxia, nutrient deprivation or matrix separation. It is also interesting to note that

under glucose deprivation both AMPK and AKT are activated and work in concert to sustain cell survival whereas under nutrient-rich conditions, the AMPK energy-sensing pathway and the PI3K/Akt cascade focus on mTOR with opposing regulatory impacts. The LKB1/AMPK pathway can therefore act as a "tumor promoter" that aims to make tumor cells more resilient to metabolic stress, especially when tumor growth exceeds the capacity of its supply of blood in order to provide nutrients and oxygen [43].

AMPK also plays an important role in preserving cells from reactive oxygen species (ROS) and the exact mechanism is still in debate. There are two theories for how ROS controls AMPK regulation. Firstly, the increased AMPK activation by H_2O_2 is increase via CaMKK2 or LKB1. S-glutathionylation of AMPKα for AMPK activation can be upregulated by glucose oxidase which generates H_2O_2. Secondly, ROS also can damage the LKB1-AMPK pathway under specific cellular conditions. Additionally, when intracellular NADPH levels are increased, fatty acid synthesis inhibition occurs to neutralize cytotoxic levels of reactive oxygen species. Therefore, ROS level, energy status and AMPK upstream kinases may influence the AMPK activity which also depends on energy conditions, cellular environment context and oxidative stress (Figure 1.5) [44].

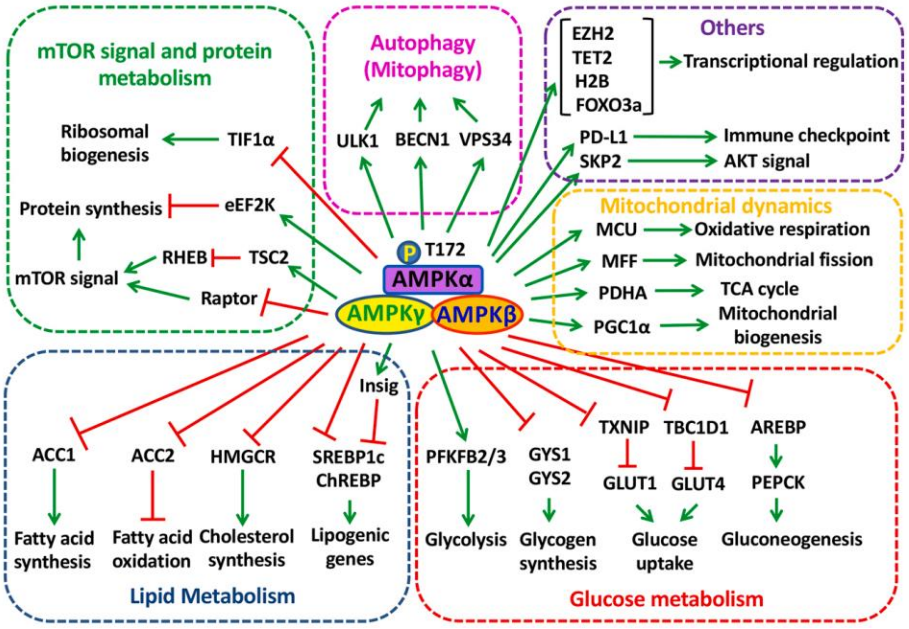

Figure 1.5. Physiological functions that are controlled by downstream substrates of AMPK.

1.3. Cell Death

Cell death is a crucial biological process for organisms and cells to grow and development. As a result of an irreversible plasma membrane integrity loss in cell death occurs through modifications in lipid metabolism in order to preserve cellular and organismal homeostasis. One the most important hallmarks of cancer cell is escaping from cell death and uncontrolled cell proliferation [45].

Dysregulation in cell death results in a variety of disease occurrence including cancer and neurodegenerative diseases. There three types of cell death that have distinctive biophysical characteristics through distinct signaling pathways which are autophagy, apoptosis, and necrosis [46].

1.3.1. Autophagy

Autophagy is an important process which degrades cellular macromolecules and organelles in order to provide recycling of intracellular bioenergetic components in response to biological stresses such as organelle damage, hypoxia, nutrient deficiency, ROS and drug therapy. The process of autophagy includes four steps which are initiation, nucleation, formation, and fusion of autophagosome with lysosome, and hydrolyzation. The creation of the autophagosome is provided by a bilayer vesicle containing damaged organelles, proteins, and other cytoplasmic elements. In addition, autophagy also can be induced by cell death or can be act as pro-survival and resistance mechanism against cancer treatment. Autophagy also play an important role in tumorigenesis. For instance, while anticancer effects of autophagy such as reduced inflammatory, genome instability and chronic tissue damage are exerted in the early stages of cancer, during the late stages, autophagy serves as an energy and nutrient supplier for growth of tumors [47].

Firstly, under low ATP condition or amino acid depletion, AMPK is activated and mTOR is inhibited. mTORC1 binds to dephosphorylate Unc-51-like kinase 1 (ULK1) to autophagy initiation as a result of ULK complex formation. To create phagophores, the membrane of ER splits and B-cell lymphoma (Bcl-2) is inhibited by phosphorylation through JNK. Then, Bcl-2 and Beclin-1 are separated to form Class III Phosphoinositide 3-kinase (PI3K) complex which interacts with ER results

in double membrane nucleation. Abnormal proteins and damaged organelles are also engulfed by phagophore. The elongation of phagophore occurs by ATG5 and ATG12 conjugation to form with ATG16L1 recruitment. The lapidated form of LC3-II is converted by the E1-like enzyme ATG7 and the E2-like enzyme ATG3 from the diffuse form of LC3-I in order to insert into the phagophore and lengthen the membrane. After mature phagosome formed, autolysosome is created with autophagosome and lysosome fusion to breakdown the cellular components (Figure 1.6.) [48].

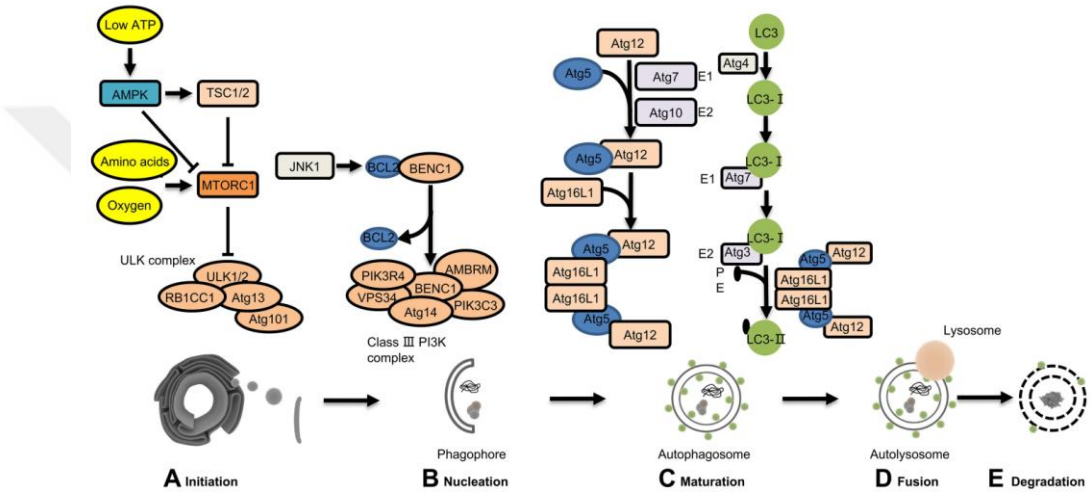

Figure 1.6. Autophagy regulation signaling pathway.

1.3.2. Apoptosis and Necrosis

Apoptosis is a type of programmed cell death that is caspase-mediated which is characterized by nuclear fragmentation, membrane blebbing and chromosome blebbing. Apoptosis also does not result in inflammation due to it is extremely controlled. The main difference between apoptosis and autophagy and necrosis is signaling in apoptosis can be triggered by death receptor which is extrinsic pathway or mitochondria which is intrinsic pathway Tumor necrosis factor α (TNF-α), TNF-related apoptosis-inducing ligand (TRAIL) or Fas ligand (CD95/APO1) result in activation of death receptor. The death-inducing signaling complex includes death receptors, adapter proteins, and caspases (cysteinyl aspartate-specific proteases) which are caspase-8 and caspase-10 in type I cells. In type II cells, caspase-3 activation is triggered by caspase-8 and cleavage of a pro-apoptotic member of the

Bcl-2 which is Bid occurred in intrinsic apoptotic pathway in order to translocation of truncated Bid to the mitochondria as well as interaction with Bax/Bak occurs that leads to cytochrome c release. Anticancer drugs, toxins and radiation can lead to activation of intrinsic pathway through mitochondrial membrane and function alterations. Cytochrome c release is influenced by permeabilization of mitochondrial membrane in order to form caspase activation complex with pro-caspase-9 and protease activating factor 1 (Apaf-1) which is called apoptosome [49]. The molecular mechanism illustration of necroptosis was shown in Figure 1.7. [51].

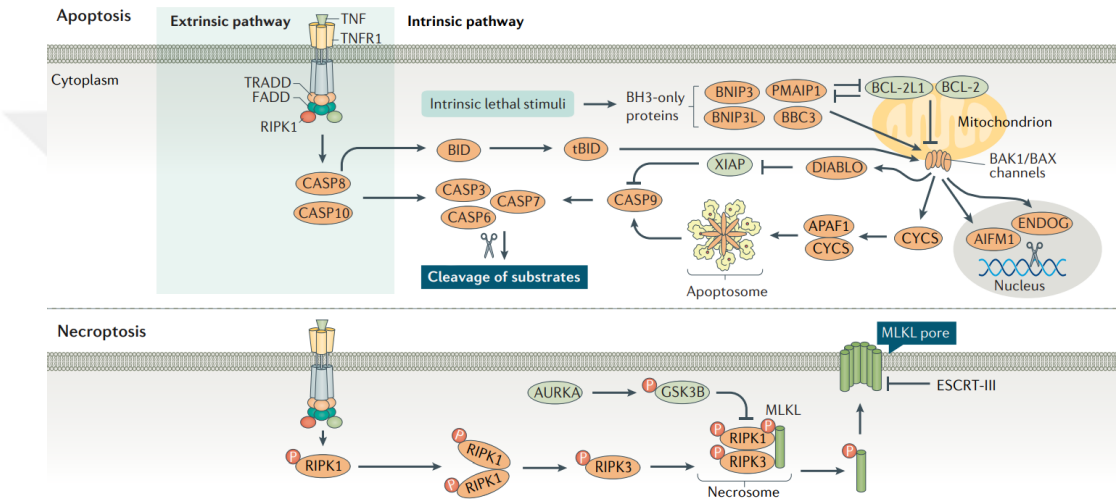

Figure 1.7. The molecular mechanism in apoptosis and necroptosis.

Necrosis is defined as accidental or unregulated cell death results from external physical damage such as detergent or mechanical stress, trauma, cell injury, toxins or infection. Enlargement organelles, rupturing in plasma membrane and inflammatory responses are the main characterization of necrosis via release of intracellular content to the extracellular environment through two main necrotic pathways: 1) death receptor pathway by TNF-α and TRAIL, 2) mitochondrial pathway through induced ROS or ATP decrease. The term “necroptosis” is defined as programmed necrosis which is similar to necrosis to that is triggered by death receptor activation during caspase inhibition. In addition, reduce in intracellular ATP also plays role in transition from apoptosis to necroptosis or necrosis which is influenced by overactivation of PARP1 via DNA damage mediation or receptor interacting serine/threonine kinase 1 (RIPK1)-dependent manner. In necroptosis, Fas ligand (FASLG) is responsible for necrosis when caspase inhibitors are present that also

requires RIPK1. Necrosome assembly occurs by phosphorylation via RIPK3 and FAS-associated via death domain (FADD) and mixed-lineage kinase domain-like pseudokinase (MLKL) recruitment. MLKL is phosphorylated through RIPK3 followed by the transportation into plasma membrane to induce membrane rupture [50]. The molecular mechanism illustration of necroptosis was shown in Figure 1.7.

1.4. *Cistus creticus*

Cistus creticus L. subsp. which is also called as Cretan rockrose is relatively small (80-100 cm high), dicotyledonous flowering in white or pink perennial herbaceous plant with hard leaves which grow mainly in the Mediterranean region especially in open areas and stony soils. The Cistus species are found in bushes above sea level in dry, sun-exposed locations and are adapted to the Mediterranean environment. The Mediterranean region of Turkey is home to 5 different species of the Cistus genus, which has 20 different species worldwide (*Cistus creticus, Cistus laurifolius L., Cistus monspeliensis L., Cistus parviflorus Lam.,* and *Cistus salviifolius L.*) [52]. An image of pink *C. creticus* is shown in Figure 1.8. [53].

Figure 1.8. Image of *Cistus creticus* (Cretan Rockrose).

1.4.1. Biological Properties of *Cistus creticus*

The essential oils extracted from *C. creticus* contain a lot of diterpenes of the labdane class. Also, a variety of non-volatile substances such as phenolic acid and flavanols are present. There are 92 terpenes and 12 distinct phenylpropanoid flavonoids found in Cistus species, especially *C. creticus* extracts are abundant in pharmacologically active compounds [54]. Typically, the leaves and stems are used to make extracts which are called Ladano. It has also been used in traditional medical applications in the eastern Mediterranean region for ages in the form of herbal tea or smoked in the treatment of various disorders like infections and digestive disorders results from abundant flavonoids, glycosides, terpenoids, and diterpenes content presence of *C. creticus*. Especially, flavonoids and polyphenols are important antioxidants to snare harmful oxygen free radicals which may contribute to the disease developments such as cancer, diabetes, and Alzheimer's disease [55].

C. creticus has a long history of use as a traditional medicinal plant for eczema, diarrhea, hair loss, furuncles, and infections. Labdanum is exudates from glandular hair of leaves and stem of the plant. Currently, a wide range of high antioxidant and polyphenol secondary compounds from *C. creticus* showed favorable health effects on respiratory diseases, influenza, and skin irritations [56].

Nowadays, the identification and isolation of bioactive compounds in *C. creticus* extracts has been studied in many scientific research due to its promising therapeutic effect on many biological diseases that show positive pharmacological activity, especially in cancer research. Cytotoxic activity of *C. creticus* extracts were studied on several cancer types such as breast, melanoma, and cervical cancer [57]. Especially, labdane type diterpenes showed the inhibitory effect as well as sclareol that is found in *C. creticus* extracts and used as certified cancer drug also showed inhibitory effects on DNA inhibition during apoptosis without the of p53 has been demonstrated which leads to cell cycle arrest [58].

1.5. Aim of the Thesis

The aim of this thesis is investigating the anti-cancer effects of ethanol and distilled water isolates of *Cistus creticus* L., grows naturally in Turkey and the Mediterranean region, which is grown under different NaCl concentrations and whose medicinal and aromatic properties have been studied variously, on pancreatic cancer cell lines. In addition, in the scope of the thesis, it is aimed to comparatively examine the therapeutic effect of *C. creticus* isolates on three different pancreatic cancer cell lines that have different mutations on cell survival, lipid metabolism, cell death, autophagy, apoptosis and necrosis.

2. MATERIALS AND METHODS

2.1. Materials

2.1.1. Cell Lines and Reagents

PANC-1 (CRL-1469), MIA PaCa-2 (CRL-1420) and AsPC-1 (CRL-1682) cell lines were purchased from American Type Culture Collection (ATCC, Rockville, MD, USA). The cells were cultured in Dulbecco's modified Eagle's medium (DMEM; GIBCO- Life Technologies, Carlsbad, CA) and Roswell Park Memorial Institute 1640 Medium (RPMI 1640; GIBCO- Life Technologies, Carlsbad, CA) supplemented with 10% fetal bovine serum (Pan Biotech GmbH, Aidenbach, Germany) and 1% penicillin/streptomycin (GIBCO, Invitrogen Co) and incubated in 37 °C with 5% CO_2 (HeraCell 150i ThermoLab systems, Beverly, MA, USA). Cell culture consumable and reagent that were used in this thesis were shown below (Table 2.1.).

Table 2.1. Cell culture consumables, cell lines and reagents.

Material Name	**Cat no. / Product no.**	**Company**
PANC-1 Cell Line	CRL-1469™	ATCC
MIA PaCa-2 Cell Line	CRL-1420™	ATCC
AsPC-1 Cell Line	CRL-1682™	ATCC
Dimethyl sulfoxide (DMSO)	1264ML250	BioFroxx
Dulbecco’s Phosphate Buffer Saline 1X (DPBS) pH: 7.4	P04-36503	PAN Biotech
Gibco™ DMEM	11965092	Life Technologies
Gibco™ Fetal Bovine Serum (FBS)	16000044	Life Technologies
Gibco™ RPMI-1640	21875034	Life Technologies
Penicillin, Streptomycin (10000 U/ml) Penicillin, 10 mg/ml Streptomycin	15140122	Life Technologies
Trypsin 0.05%/EDTA 0.02% in DPBS	P10-0231SP	PAN Biotech

2.1.2. Laboratory Equipment and Devices

Laboratory equipment and devices that were used in the thesis shown in Table 2.2.

Table 2.2. List of laboratory equipment and devices that were used during this thesis.

Product Name	Model/Cat no.	Company
+4°C refrigerator	454270	Arçelik
0.22 µm filter	7101451	GVS
0.45 µm filter	7091543	GVS
10 µL pipette	7030301004	DLAB
10 µL tips	5130010C	CAPP
1000 µL pipette	7030301016	DLAB
1000 µL tips	5130130C	CAPP
15 ml centrifuge tubes	5100015C	CAPP
200 µL pipette	7030301009	DLAB
200 µL tips	5130070C	CAPP
-20°C freezer	FLV1003	Flavel
24-well plate	92024	TPP
3D orbital shaker	WT 12	BIOMETRA
50 ml centrifuge tubes	5100050C	CAPP
6-well plate	92006	TPP
-80°C freezer	DF490	Nüve
96-well plate	92096	TPP
Analytical balance	1200C	PRECISA
Autoclave machine	Hiclave HVE 50	HIRAYAMA
Autoclave machine	Hiclave HV 110L	HIRAYAMA
ChemiDoc XRS+ Imaging System	1708265	Bio-Rad Laboratories
Cooling micro centrifuge machine	D1524R	DLAB
Cryotube	190321	Microcult
Drying oven	Z603945	BINDER ED115
Forma™ Steri-Cycle™ i160 CO_2 Incubator CO2	51030301	Thermo Scientific

Table 2.2. Continued.

Heat Block	5032141212	DLAB
Hemocytometer	0640010	Marienfeld
Ice maker machine	GB 601	BREMA Ice Flaker
Inverted microscope	ICX41	SOIF
Magnetic stirrer	8030261100	DLAB
Microcentrifuge tubes	5100505C	CAPP
Mini Blot Transfer Module	B1000	Invitrogen
Mini Gel Western Blot Tank	A25977	Invitrogen
pH meter	HI-2002-02	HANNA
PowerEase™ Touch Power Supply	PS0351	Invitrogen
Safe 2020 Class II Biological Safety Cabinet	51026638	Thermo Fisher Scientific
Spin	HB20CAV00 05823	DLAB
Sterile syringe	86999317540 32	Genject
Tissue Culture Flasks 25	90026	TPP
Tube roller	MX-T6-S/S+	DLAB
Varioskan™ LUX multimode microplate reader	VL0000D0	Thermo Fisher Scientific
Vortex	8031102000	DLAB
Waterbath	M 24 K	Electromag
WesternBright PVDF-CL Transfer Membrane	L-08024-001	Advansta
ZOE fluorescent cell imager	1450031	Bio-Rad Laboratories

2.1.3. Chemicals and Solutions

All the chemicals and solutions that were used in this thesis were shown in Table 2.3.

Table 2.3. List of chemicals and solutions that were used during this thesis.

Product Name	Cas no. / Lot no.	Company
4X Bolt™ LDS Sample Buffer	B0007	Invitrogen
Acetic acid	27225	Sigma-Aldrich
BODIPY 493/503	121207-31-6	Sigma-Aldrich
Bradford Reagent	BR05/BR0422	Clear Band
CM-H2DCFDA (General Oxidative Stress Indicator)	C6827	Invitrogen
DAPI	28718-90-3	BioShop
DiOC6	2129966	Fluka
Ethanol	64-17-5	Sigma-Aldrich
Luminol	A2185	PanReac AppliChem
LysoTracker™ Red DND-99	L7528	Invitrogen
Methanol	24229	Sigma-Aldrich
MitoTracker™ Red CMXRos	M7512	Invitrogen
M-PER Mammalian Protein Extraction Reagent	78501	Thermo Scientific
Bolt™ Bis-Tris Plus Mini Protein Gels, 4-12%, 1.0 mm	NW04122BOX	Invitrogen
PageRuler™ Plus Prestained Protein Ladder	26619	Thermo Scientific
Propidium iodide	P3566	Invitrogen
Skim Milk powder	5E81FA7E	BioFroxx
Thiazolyl blue tetrazolium bromide (MTT)	1334GR001	BioFroxx
Trans-4- Hydroxycinnamic acid	10221426	Alfa Aesar
Tris-Base	77-86-1	BioShop
Tris-HCl	1185-53-1	BioShop
Tween-20	0B64696	BioShop

2.2. Methods

2.2.1. Plant Material and Extraction of *Cistus creticus*

Hairy labdanum (*Cistus creticus* L.) seeds were collected from the forest in the Derince district of Kocaeli, Turkey, in 2020. The plants were grown by the Department of Biotechnology's Plant Physiology and Nutrition Laboratory at Gebze Technical University (Kocaeli, TR) during the spring and summer of 2021. Three different salt concentrations (0, 30 and 60 mM) were applied to the plants. After the growing period, the plant's shoots and roots were collected separately and dried for two days at 70 °C.

The plant samples were extracted by using two different solvents (70% EtOH and dH_2O). For the extraction, 30 ml of dH_2O and 70% EtOH were mixed with 5 grams of dried and finely ground plant material. The mixture was then shaken at room temperature for an hour. In a filtered glass crucible, the extract was filtered under a vacuum. The plant samples left on the filter twice were filtered by gradually adding 15 ml of 70% EtOH. Extracts were dried for 1 hour at 35–40 °C, 75 rpm, and 40 mbar absolute pressure in the rotary evaporator's water bath. Extracts were further dried for 24 hours in an oven set at 40 °C. dH_2O and EtOH were used to dilute each extract. The extracts were sonicated until they were all completely dissolved. In pre-weighted centrifuge tubes, the solutions were centrifuged at 5000 rpm for 15 minutes at 4°C. The final precipitates were weighed and recorded, and the supernatants were collected. The final step involved adjusting the concentration of the supernatants to 100 mg/ml by using dry matter calculations, and then adding 70% EtOH or dH_2O. Before being used for analysis, the samples were aliquoted and kept at a temperature of -20 °C.

2.2.2. Cell Culture

PANC-1 (CRL-1469), MIA PaCa-2 (CRL-1420) and AsPC-1 (CRL-1682) cell lines were purchased from American Type Culture Collection (ATCC, Rockville, MD, USA). MIA PaCa-2 and PANC-1 cells were cultured in Dulbecco's modified Eagle's medium (DMEM) and AsPC-1 cells were cultured in Roswell Park Memorial

Institute 1640 Medium (RPMI-1640) supplemented with 10% fetal bovine serum and 1% penicillin/streptomycin and cells were incubated in 37 °C with 5% CO_2. Passaging of cells was followed and observed by inverted microscope and cell growth media were changed in every 2-3 days intervals depending on their growth rate.

70% ethanol and distilled water extracts of *Cistus creticus* were obtained from Department of Biotechnology, Plant Physiology and Nutrition Laboratory, Gebze Technical University (Kocaeli, TR) and stored at an initial stock concentration of 10 mg/ml as aliquots at -20°C until they were used for analyses.

2.2.3. Cell Thawing

Frozen cell lines with freezing media containing (90% FBS-10% DMSO) in -80ºC cryotubes were quickly thawed and the cells were transferred to centrifuge tubes by adding medium at 1:5 ratio. Cells were centrifuged at 1500 rpm for 5 minutes. By that, negative effect of DMSO on cell viability was quickly reduced. After centrifugation, the supernatant was removed, and the pellet was dissolved with the growth media. Cells were cultivated by placing 3 ml of complete media in T25 and were placed in 37 °C with 5% CO_2 incubator. The media was changed every 2 days until the cells reached the confluency.

2.2.4. Cell Freezing

The cells that had proliferated by adhering to the surface in T25 cell culture flask were removed enzymatically from the surface to which the cells were adhered, with the help of 500 µl of trypsin-EDTA. Trypsin-EDTA activity was inhibited with 1 ml of complete medium, and then the cells were collected into sterile falcon tubes and precipitated by centrifuging at 1500 rpm for 5 minutes. Cells were suspended with growth media and counted with the help of Neubauer hemocytometer. After the cells were counted, they were mixed with the freezing media containing FBS-DMSO prepared at a ratio of 9:1 into the cryotubes. The freezing method, which was carried out for the preservation of cells with low passage numbers, cells were kept in a freezer at -80ºC.

2.2.5. Dose-Dependent Cell Viability Assay (MTT Assay)

The effects of the *C. creticus* extracts on pancreatic cancer cell lines' viability were determined by a colorimetric MTT (3-(4,5-dimethylthiazol-2-yl)-2,5-diphenyltetrazolium bromide) assay. The assay was based on the colorimetric method of detecting the color change seen as a result of the production of formazan salt (purple) by cleaving the tetrazolium ring of the MTT spacer (yellow) with the increased dehydrogenase enzyme in living and mitochondrial intact cells. Cells were seeded at a density of $1x10^4$ cells per well in 96-well plates. After the cells adhered to the plate, they were treated with three different concentrations (125 µg/ml, 250 µg/ml and 500 µg/ml) of each three different salt concentrations of *C. creticus* extracts (0, 30, 60 mM of NaCl) through ethanol and water extraction methods for 24 h. Then, 10 µL of MTT reagent (5 mg/ml) was added to the culture media and incubated at 37°C for 4 h. After 4 hours, the media with MTT reagent was removed from the cells. To solubilize the formazan crystals converted from MTT by the mitochondrial enzymes, 100 µl dimethyl sulfoxide (DMSO) was added to each well and shaken gently for 15 minutes in the dark. After incubation, the absorbance of the suspension at 570 nm was measured in a microplate reader.

2.2.6. Colony Formation Assay

The pancreatic cancer cells were seeded at a density of 3 × 103 cells/well in 6-well plates and allowed to adhere for 24 h. After attachment, the cells were treated with increasing concentrations of 70 %EtOH extracts of 60 mM NaCl-treated *C. creticus* (50, 100, 125, 250 and 500 µg/ml) and distilled water extracts of 60 mM NaCl-treated *C. creticus* (50, 100, 125, 250 and 500 µg/ml) for 24 h. After 24 h, the culture media were removed, and the cells were allowed to form colonies in complete media for 10 days. The medium was renewed every three days. After colonies were formed, culture media was removed and washed twice with 1X PBS. For colony fixation, 1 ml of the acetic acid/methanol (1:3) solution was added to each well and fixed for 5 minutes. After 5 minutes, acetic acid/methanol mixture was removed, and the cells were stained with 500 µl of 0.5% crystal violet for 30

minutes. Excess dye residues were removed from the cells and washed with distilled water. The image of visible colonies in each well was taken with a camera.

2.2.7. The Reactive Oxygen Species (ROS) Assay through Fluorescence Spectroscopy

3×10^4 cells per well were seeded in 24-well plates and treated with selected doses of 125 µg/ml, 250 µg/ml, and 500 µg/ml of each three different salt concentrations (0, 30, 60 mM NaCl) of *C. creticus* extracts through ethanol extraction method for 24 h. After 24 hours of treatment, the cells were washed with 1X phosphate buffered saline (PBS) and were stained with CM-H2DCFDA dye diluted in serum-free culture medium (1:1000), and cells were incubated for 30 minutes at 37℃ in a 5% CO2 incubator. Later, fluorometric measurement of reactive oxygen species was analyzed by Varioskan™ LUX multimode microplate reader. (Ex/Em:492/517 nm).

2.2.8. Visualization of Mitochondrial Membrane Potential by MitoTracker™ Red CMXRos Staining with Fluorescence Microscopy

Pancreatic cancer cells were seeded at a density of 3×10^4 cells per well in 24-well plates and waited to adhere to the surface. After cell adhesion to the surface, the cells were treated with selected doses of 125 µg/ml, 250 µg/ml and 500 µg/ml of each three different salt concentrations (0, 30, 60 mM NaCl) of *C. creticus* extracts through ethanol and water extraction method for 24 h. After 24 hours of treatment, the cells were washed with 1X phosphate buffered saline (PBS) and were stained with 500 µl MitoTracker™ Red CMXRos dye diluted as 1:1000 in serum-free culture medium for each well. Then, the cells were incubated 30 minutes at 37 ℃ in a 5% CO_2 incubator. After incubation, subcellular mitochondrial mass and oxidative activity of live cells were visualized and images of cells were taken with ZOE fluorescent microscope at 100 µm scale bar.

2.2.9. Detection of Lipid Droplets by BODIPY® 493/503 Staining and Visualization of Nucleus by 4',6-diamidino-2-phenylindole (DAPI) with Fluorescence Microscopy

Pancreatic cancer cells were seeded in 24-well plates at a density of $3x10^4$ cells per well. After cell adhesion to the surface, the cells were treated with selected doses of 250 µg/ml and 500 µg/ml of two different salt concentrations (30 and 60 mM NaCl) of *C. creticus* extracts through ethanol extraction method for 24 h. After 24 hours of treatment, the cells were washed with 1X phosphate buffered saline (PBS) and were stained with 500 µl BODIPY® 493/503 and 5 mg/ml DAPI dye diluted as 1:1000 in serum-free culture medium for each well. Then, the cells were incubated 20 minutes at 37 ℃ in a 5% CO_2 incubator. After incubation, subcellular lipid droplets by BODIPY as green color and DNA condensation in nucleus due to DNA breaks of cells by DAPI as blue color were visualized and images of cells were taken with ZOE fluorescent microscope at 45 µm scale bar.

2.2.10. Detection of Cell Death and Mitochondrial Membrane Potential by PI and DiOC6 Staining in Fluorescence Microscopy

Pancreatic cancer cells were seeded in 24-well plates at a density of $3x10^4$ cells per well. After cell adhesion to the surface, the cells were treated with selected doses of 125 µg/ml, 250 µg/ml and 500 µg/ml of each three different salt concentrations (0, 30, 60 mM NaCl) of *C. creticus* extracts through ethanol extraction method for 24 h. After 24 hours of treatment, the cells were washed with 1X phosphate buffered saline (PBS) and were stained with 500 µl Propidium Iodide (PI) and 3,3′-Dihexyloxacarbocyanine iodide (DiOC6) dye diluted as 1:1000 in serum-free culture medium for each well. Then, the cells were incubated 20 minutes at 37 ℃ in a 5% CO_2 incubator. After incubation, dead cells were observed at 536 nm excitation and 617 nm emission as red color by PI and cells with healthy mitochondria potential were observed at 488 nm excitation and 525 nm emission as green color. Images of cells were taken and visualized by using ZOE fluorescent microscope at 100 µm scale bar.

2.2.11. Detection of Protein Expression Levels by Western Blotting

2.2.11.1. Total Protein Isolation

Pancreatic cancer cells PANC-1, MIA PaCa-2 and AsPC-1 cells were seeded in 6-well plates as 3×10^5 cells per well and incubated overnight in a 37 °C and 5% CO_2 incubator for cell adhesion. Cells were treated with a selected doses of 500 µg/ml EtOH extract and 500 µg/ml H_2O extract of 60 mM NaCl-treated *C. creticus* for 24 h. Following the drug treatment, culture media were removed from cells and cells were washed two times with ice-cold 1 ml 1X PBS. Cells were lysed on ice with an appropriate (150-200 µl) amount of protein lysis solution (M-PER Mammalian Protein Extraction Reagent) and shaken gently for 20 minutes at 4°C. After the lysis procedure, cells were scraped and transferred into 1.5 ml microcentrifuge tubes. Then, cell debris was removed by centrifugation at 14,000 × g for 10 minutes at +4°C. After centrifugation, the supernatant was transferred into new 1.5 ml microcentrifuge tubes for protein concentration measurement.

2.2.11.2. Determination of Protein Concentration with Bradford Assay

The Bradford assay was used to determine the protein concentration. The standard curve was first created using bovine serum albumin (BSA) with a stock concentration of 2 mg/ml by preparing increasing amounts of BSA concentrations as 25 µg/ml, 125 µg/ml, 250 µg/ml, 500 µg/ml, 750 µg/ml, 1000 µg/ml, 1500 µg/ml and 2000 µg/ml BSA, respectively. 2 µl of each BSA solutions and blank were added in 96 well plate and incubated with 100 µl Bradford Reagent for 10 minutes at room temperature. Absorbance measurement was performed at 595 nm by microplate reader. After standard curve preparation, 2 µl of M-PER protein isolation solution was used as blank and 2 µl from each isolated protein samples were placed into 96-well plates on ice and 100 µl Bradford reagent was added onto protein samples and incubated for 10 minutes at dark. After incubation, absorbance measurement at 595 nm was performed in microplate reader and protein concentrations were calculated according to standard curve.

2.2.11.3. Sample Preparation and Gel Electrophoresis

20 µg protein samples from each protein lysates were mixed with 4X LDS sample buffer as 1:4 ratio to denature and to linearize proteins in 1.5 ml microcentrifuges tubes and were incubated at 70°C for 10 minutes by heat block. After denaturation step, 2 µl protein ladder and protein samples were loaded in 12% polyacrylamide Bis-Tris mini gel. Gel was placed in the tank and a 1X running buffer was poured into the tank. Gel was run at 80-120 V with 1X running buffer for 50-80 minutes.

2.2.11.4. Protein Transfer into PVDF Membrane

After gel electrophoresis, polyvinyl fluoride (PVDF) membrane to be used was activated with methanol for 10 seconds and washed with distilled water for 10 seconds. Sandwich transfer model was created between pre-soaked sponge pads and filter papers with 1X transfer buffer, vertically. The transfer module was placed into a mini gel tank and transfer cassette filled with 1X transfer buffer. Then, the transfer module was soaked with distilled water and proteins were transferred at constant voltage of 20V for 60 minutes.

2.2.11.5. Membrane Blocking and Antibody Incubation

After the transfer process, PVDF membrane was blocked with 5% skim milk/1X TBS-T (Tris-buffered saline containing 0.1% Tween 20) for 1 hour at room temperature. After, membrane blocking process, the membrane was washed with 1X TBS-T for 5 minutes and incubated with selected primary antibody (1:1000 in 5% skim milk/1X TBS-T) overnight at +4^{o}C. After primary antibody incubation, membrane was washed three times with 1X TBS-T for 10 minutes and the membrane was incubated with horseradish peroxidase (HRP)-linked secondary antibody (1:1000 in 5% skim milk/1X TBS-T) compatible with primary antibody for 1 hour at room temperature. Then, the membrane was washed twice with 1X TBS-T and washed once with 1X TBS for 5 minutes.

Used monoclonal antibodies; Autophagy Antibody Sampler Kit #4445, Human Reactive Cell Death and Autophagy Antibody Sampler Kit #42867, Fatty Acid and Lipid Metabolism Antibody Sampler Kit #8335, mTOR Pathway Antibody Sampler Kit #9964, Rag and LAMTOR Antibody Sampler Kit #8665 and β-Actin (D6A8) (HRP Conjugate) #12620 antibodies were purchased from Cell Signaling Technology.

2.2.11.6. Protein Detection and Visualization

Enhanced chemiluminescence (ECL) solution was prepared to detect and quantify proteins on membrane. After the membrane was incubated in ECL solution for 1 minute at dark, chemiluminescent irradiations were detected and visualized by ChemiDoc™ XRS+ Imaging System.

2.2.12. Statistical Analysis

Standard deviation for MTT cell viability data and ROS assay data was calculated by Microsoft® Excel® for Microsoft 365 MSO (Version 2304). The significance of the effects of the treatments for each experiment was evaluated by using analysis of variance (ANOVA). Western blot quantification was performed by Image J software.

3. RESULTS

3.1. Ethanol extracts of *C. creticus* reduced cell viability and proliferation in a dose-dependent manner.

The effects of the ethanol and water extracts of *C. creticus* on relative cell viability of pancreatic cancer cell lines were determined by a colorimetric MTT assay. MTT cell viability assay of pancreatic cancer cells was proceeded to evaluate cytotoxic responses against three different concentrations (125 μg/ml, 250 μg/ml, and 500 μg/ml) of each three different salt concentrations of *C. creticus* extracts (0, 30, 60 mM of NaCl) through EtOH and water extraction method for 24 h, which was shown in Figure 3.1.

Considering the PANC-1 cells, it was shown that both ethanol and water extraction methods inhibited cell viability significantly due to increasing doses. Especially, 500 μg/ml remarkably reduced cell viability by almost 60-70% compared to control group. Ethanol extracts of each NaCl-treated plants (0, 30 and 60 mM) showed better cytotoxicity response then water extracts.

Considering MIA PaCa-2 cells, 500 μg/ml of all the EtOH extracts showed a significant cytotoxicity on cell viability compared to control group as down to 60-70 % decrease. 500 μg/ml of all the water extracts showed a significant cytotoxicity on cell viability compared to control group as 30-50% decrease. As a result of this, ethanol extracts inhibited relative cell viability better than water extracts. However, significant effect on cell viability could not be observed until 250 μg/ml. After 250 μg/ml of all extract treatment, relative cell viability was decreased in MIA PaCa-2 cells.

Considering AsPC-1 cell line, it was shown that relative cells viability started to decrease after 250 μg/ml dosage for all EtOH and water extracts. EtOH and water extracts showed similar cytotoxicity effects on cell viability for all NaCl-treated plant extracts. Cell viability slightly increased in AsPC-1 cells for 125 μg/ml and 250 μg/ml and then decreased after the dose of 250 μg/ml. 500 μg/ml of both EtOH and water extracts remarkably reduced cell viability by almost 70-80% compared to control group.

Considering all the pancreatic cancer cell lines (PANC-1, MIA PaCa-2 and AsPC-1), ethanol extracts of *C. creticus* had the most effective cytotoxicity inhibition in every concentration of NaCl-treated plants, according to Figure 3.1. The most common effective inhibition was observed in 0 mM and 60 mM NaCl-treated *C. creticus* plants.

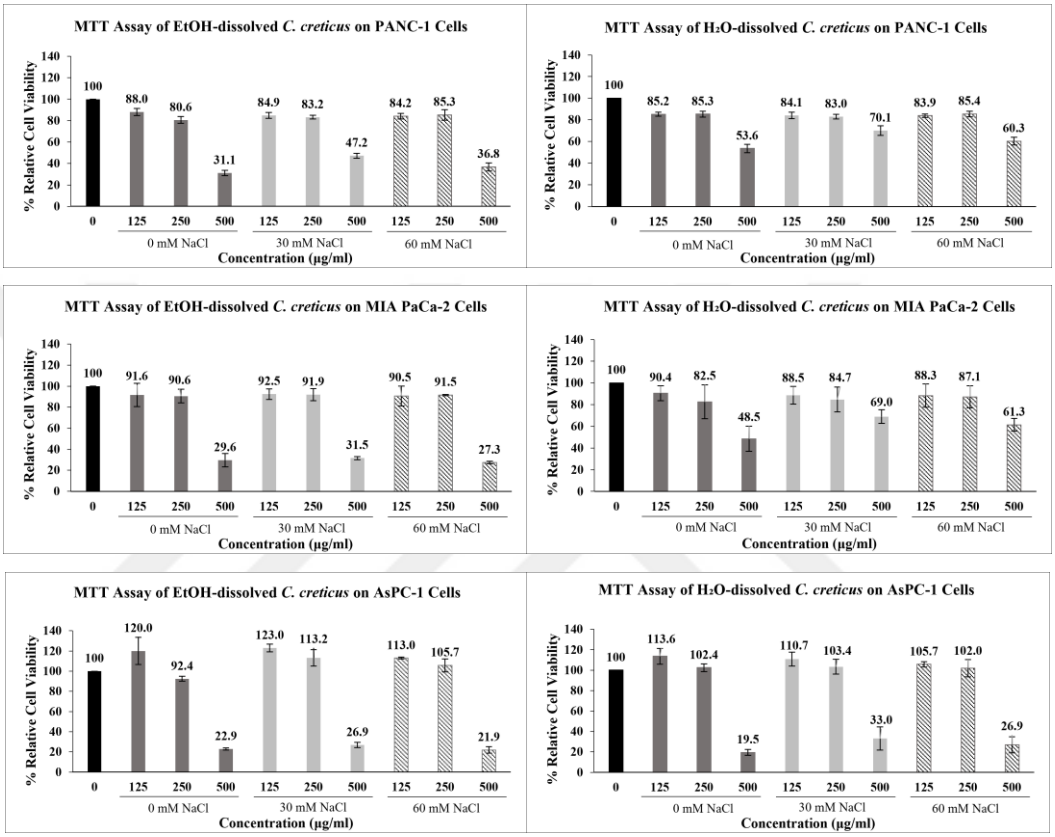

Figure 3.1. MTT cell viability assay of pancreatic cells lines proceeded to evaluate cytotoxic responses against three different concentrations (125 µg/ml, 250 µg/ml and 500 µg/ml) of three different salt concentrations of *C. creticus* extracts (0, 30, 60 mM of NaCl) through ethanol and water extraction method for 24 h. Columns represent the mean ± Std. dev of three independent experiments with at least four repeats.

Colony formation assay was performed to observe colony forming abilities of pancreatic cancer cell lines from a single cell. Pancreatic cancer cells were exposed to increasing concentrations of ethanol and water extracts (50, 100, 150, 250 and 500 µg/ml of 60 mM NaCl-treated *C. creticus)* for 24 h. A significant decrease in the colony-forming ability of cells was observed after 100 µg/ml concentration for EtOH extraction method and a significant decrease in the colony-forming ability of cells was observed after 150 µg/ml concentration for water extraction method for all the

cell lines compared to control group. In addition, 150, 250 µg/ml and 500 µg/ml showed a more effective therapeutic effect in suppressing the colony formation in PANC-1 and AsPC-1 cell lines compared to MIA PaCa-2 cells for ethanol extracts PANC-1 and AsPC-1 cells were more sensitive to treatment regarding colony-forming ability and colony formation ability of MIA PaCa-2 cells were suppressed after the dose of 150 µg/ml, which was shown Figure 3.2.

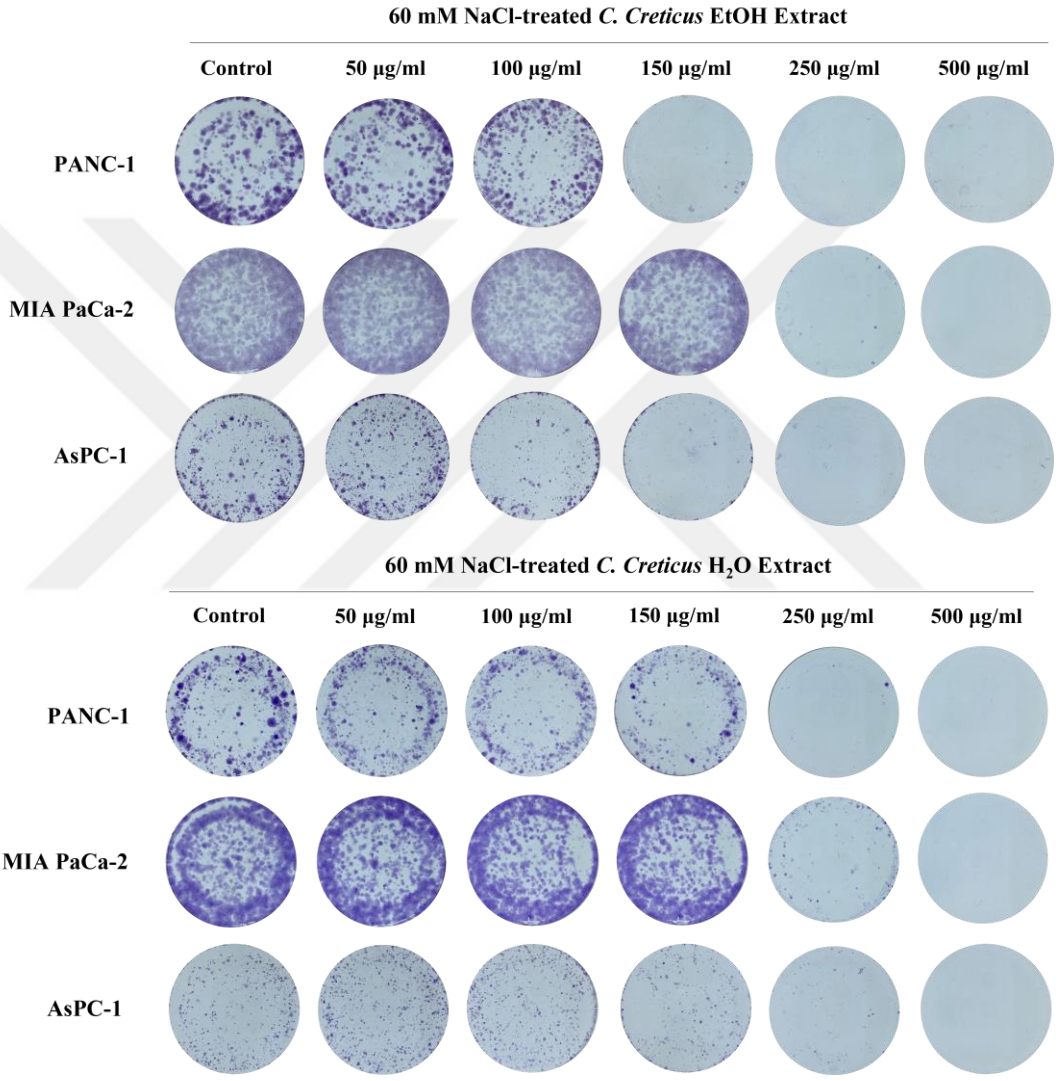

Figure 3.2. PANC-1, MIA PaCa-2 and AsPC-1 cells were exposed to 50, 100, 150, 250 and 500 µg/ml of high salt (60 mM) *Cistus creticus* extracts through ethanol (EtOH) and distilled water (dH_2O) extraction for 24 h, respectively. Then, the colony formation of cells was counted after 12 days of treatment with media replenishment every 2 days. The representative image is taken from two independent replicates.

As a result of MTT cytotoxicity assay and colony formation assay, 250 μg/ml and 500 μg/ml of ethanol extracts were determined as selected doses for further applications of this thesis (Figure 3.1. and Figure 3.2.).

3.2. Ethanol extracts of *C. creticus* eliminated ROS through reduced mitochondrial activity.

Reactive oxygen species detection in pancreatic cancer cells against three different concentrations (125 μg/ml, 250 μg/ml, and 500 μg/ml) of each three different salt concentrations of *C. creticus* extracts (0, 30, 60 mM of NaCl) through ethanol extraction method were measured after 24 h of treatment period. Intracellular ROS levels decreased with the increasing concentrations of extracts for all PDAC cell lines. Considering all the PDAC cell lines, 500 μg/ml was the most effective to decrease intracellular ROS levels compared to control group. The most effective results to suppress ROS levels were observed in MIA PaCa-2 and PANC-1 cells, respectively. Similar results were observed in AsPC-1 cells for all NaCl concentrations. 0 mM and 60 mM NaCl-treated ethanol extracts of *C. creticus* was more effective than 30 mM NaCl-treated ethanol extracts to decrease intracellular ROS levels, which was shown in Figure 3.3.

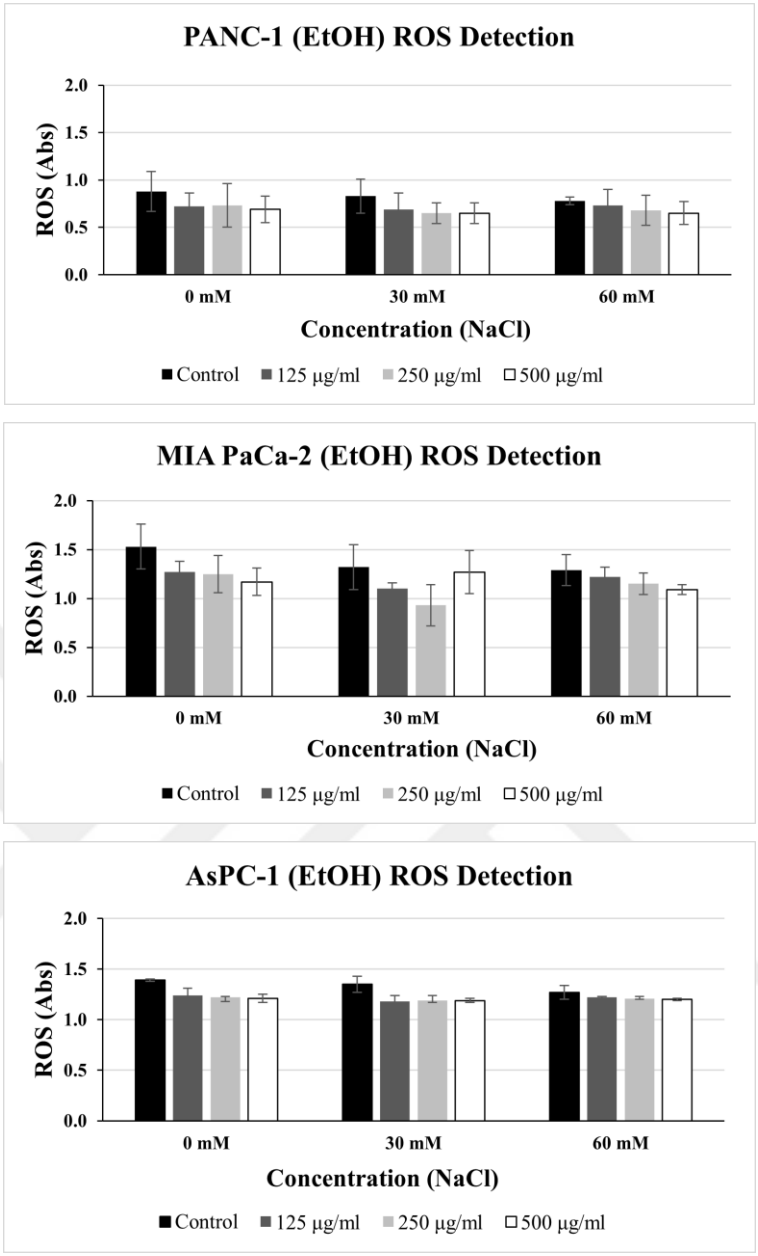

Figure 3.3. ROS detection of PANC-1, MIA PaCa-2 and AsPC-1 cells against three different concentrations (125 µg/ml, 250 µg/ml and 500 µg/ml) of each three different salt concentrations of *C. creticus* extracts (0, 30, 60 mM of NaCl) through ethanol extraction method for 24 h. Fluorometric measurement was performed by CM-H2DCFDA (General Oxidative Stress Indicator) with E_x/E_m: 492/517 nm. Columns represent the mean ± Std. dev of two independent experiments with four technical replicates.

Mitochondrial changes by MitoTracker Red CMXRos fluorescence signals in pancreatic cancer cells were observed. Cells were exposed to three different concentrations (125 µg/ml, 250 µg/ml and 500 µg/ml) of each three different salt concentrations of *C. creticus* extracts (0, 30, 60 mM of NaCl) through the EtOH

extraction method for 24 h. The concentration of 250 μg/ml of 0 mM and 60 mM NaCl-treated *C. creticus* ethanol extracts were more effective in MIA PaCa-2 and AsPC-1 cells to suppress mitochondrial activity. The most significant decrease in mitochondrial activity and function depending on membrane potential was observed in MIA PaCa-2 and AsPC-1 cells with a concentration of 250 μg/ml, respectively in EtOH extraction.

Considering water extraction, mitochondrial activity decreased effectively in PANC-1, MIA PaCa-2 and AsPC-1 cells respectively and a slight decrease was observed after 250 μg/ml concentration of treatment whereas considering ethanol extraction, a significant decrease was observed in mitochondrial activity after 125 μg/ml concentration. 30 mM NaCl-treated plant had the least effect on decreasing mitochondrial activity among other experimental groups.

Thus, ethanol extracts of *C. creticus* were selected for further experiments.

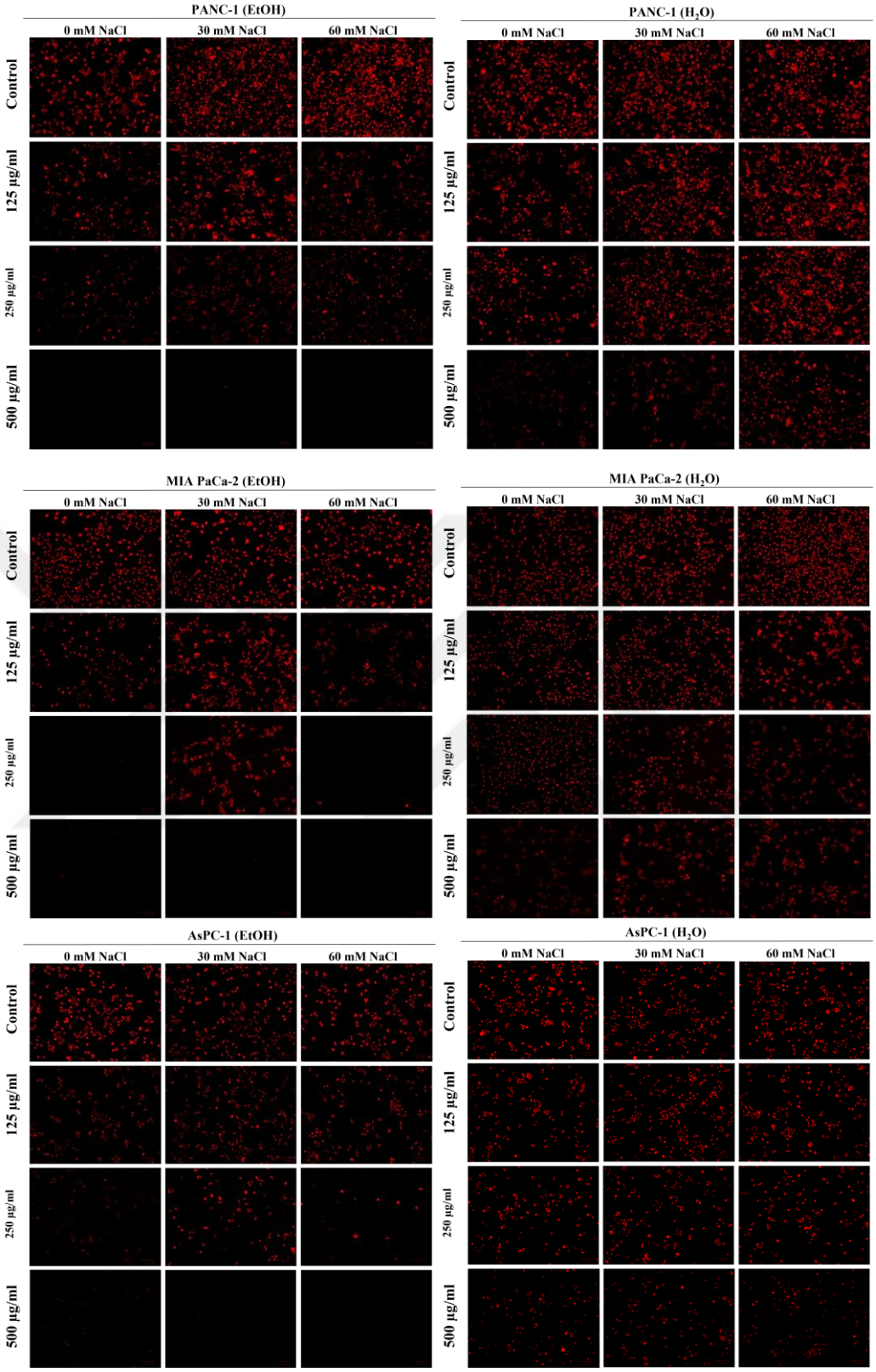

Figure 3.4. Mitochondrial changes by MitoTracker Red CMXRos fluorescence signals. Mitochondrial changes in PANC-1, MIA PaCa-2 and AsPC-1 cells, respectively. Cells were exposed to three different concentrations (125 µg/ml, 250 µg /ml, and 500 µg/ml) of each three different salt concentrations of *Cistus creticus*

extracts (0, 30, 60 mM of NaCl) through ethanol extraction method and water extraction method for 24 h (Scale bar = 100 μm).

3.3. Ethanol extracts of C. *creticus* grown under different salinity stresses triggered cell death by disrupting the mitochondrial membrane potential in pancreatic cancer cell lines.

Changes in mitochondrial membrane potential by DiOC6 and dead cells of DNA in nucleus by propidium iodide (PI) were performed. PANC-1, MIA PaCa-2 and AsPC-1 cells were exposed to 250 μg/ml and 500 μg/ml of each three different salt concentrations of *C. creticus* extracts (0, 30, 60 mM of NaCl) through the EtOH and water extraction methods for 24 h.

In PANC-1 cells, 0 mM and 30 mM NaCl-treated plant extracts showed similar effect on decreasing mitochondrial membrane potential at the 250 μg/ml and 500 μg/ml concentrations. It was observed that mitochondrial membrane potential fluorescence signals were significantly decreased with the increasing concentrations of all salinity stress groups. 60 mM NaCl-treated plant extract remarkably decreased the mitochondrial membrane potential. PI fluorescence signals were increased with increasing concentrations. Increasing number of dead cells were observed with increasing concentrations of all salinity stress groups. 500 μg/ml of 60 mM NaCl-treated plant extract was the most effective on increasing the cell death by disrupting mitochondrial membrane potential which was shown in Figure 3.5.

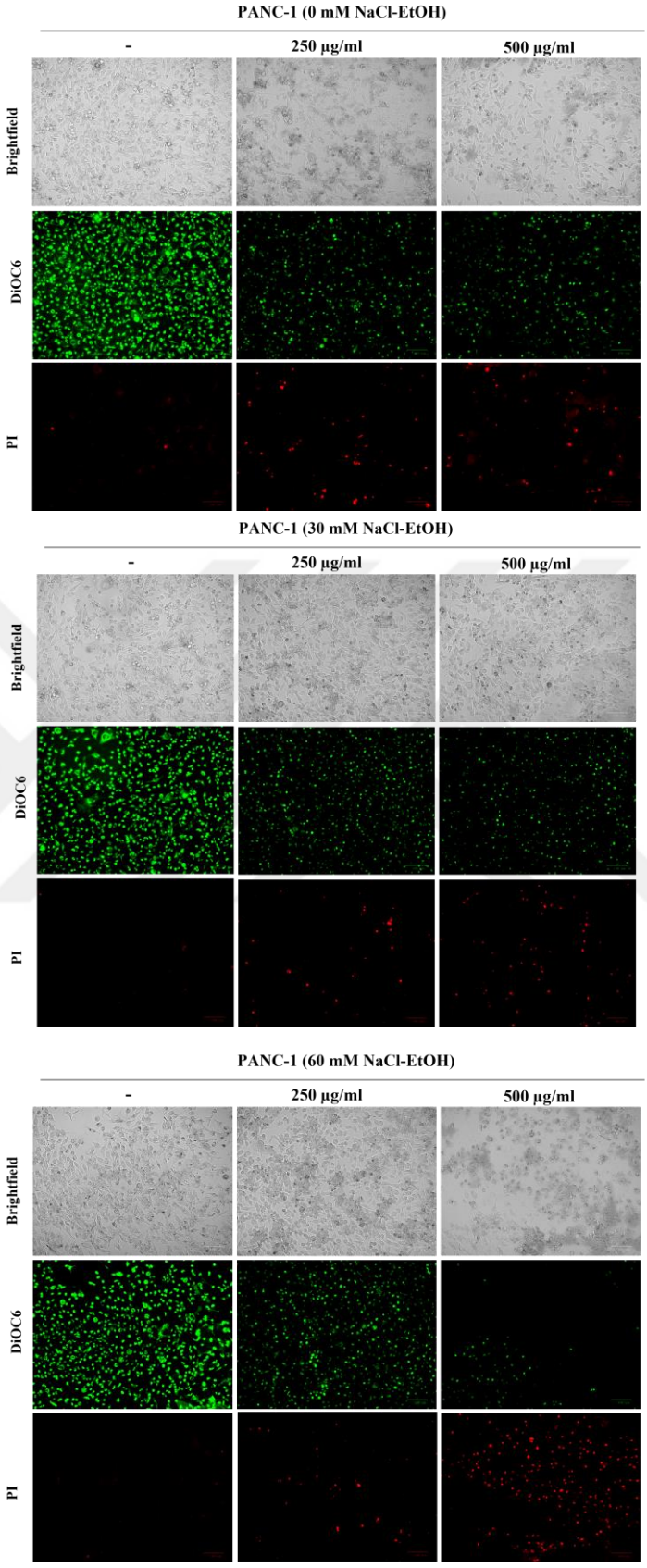

Figure 3.5. Fluorescence signals of mitochondria of live cells by DiOC6 (3,3'-Dihexyloxacarbocyanine Iodide) and DNA in apoptotic cells by Propidium Iodide (PI) in PANC-1 cells. Cells were exposed to 125µg/ml, 250 µg/ml and 500 µg/ml of

0 mM, 30 mM and 60 mM NaCl-treated ethanol extracts of C*istus creticus*, respectively for 24 h (Scale bar = 100 μm).

In MIA PaCa-2 cells, 0 mM and 60 mM NaCl-treated plant extracts showed similar effect on decreasing mitochondrial membrane potential at the 250 μg/ml and 500 μg/ml concentrations. It was observed that mitochondrial membrane potential fluorescence signals were significantly decreased with the increasing concentrations of all salinity stress groups. The least effect on decreasing mitochondrial membrane potential was observed in 30 mM NaCl-treated plant extracts. 0 mM and 60 mM NaCl-treated plant extract remarkably decreased the mitochondrial membrane potential. PI fluorescence signals were increased with increasing concentrations. Increasing number of dead cells were observed with increasing concentrations of all salinity stress groups. 500 μg/ml of 30 mM and 60 mM NaCl-treated plant extract was the most effective on increasing the cell death by disrupting mitochondrial membrane potential which was shown in Figure 3.6.

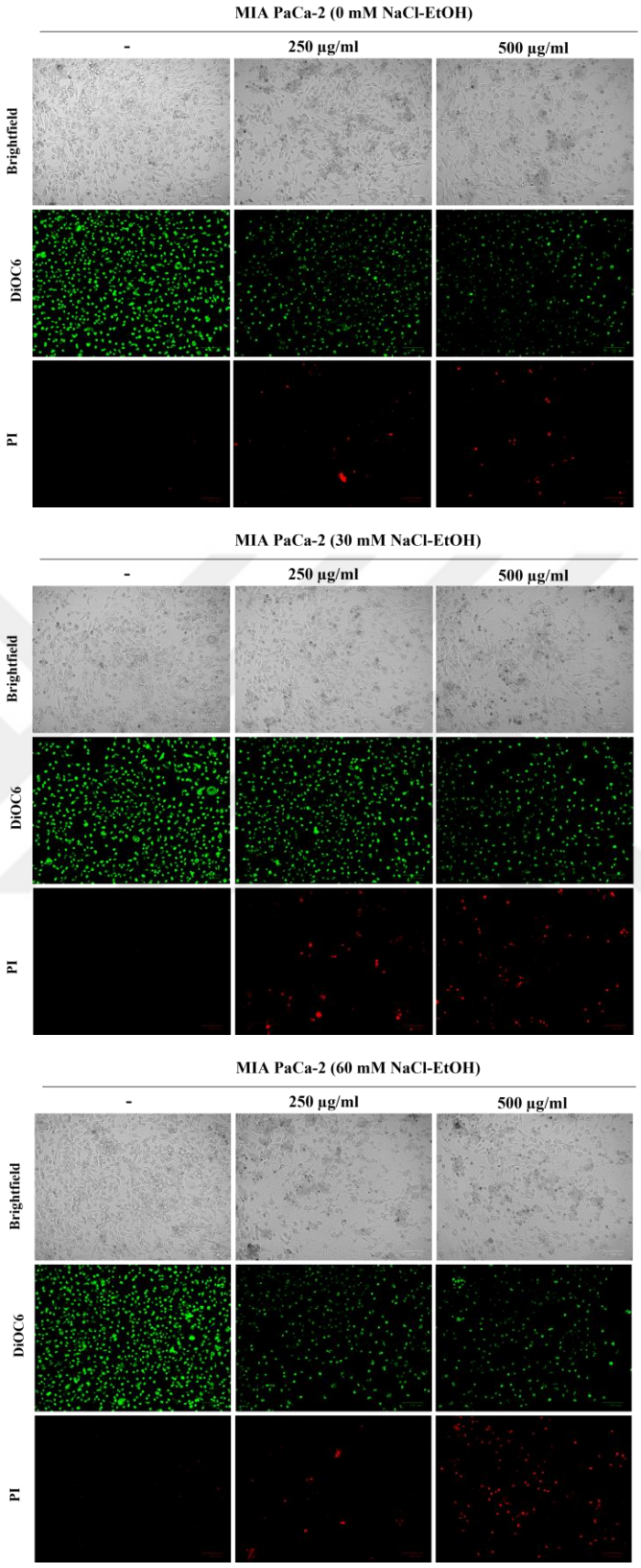

Figure 3.6. Fluorescence signals of mitochondria of live cells by DiOC6 (3,3'-Dihexyloxacarbocyanine Iodide) and DNA in apoptotic cells by Propidium Iodide

(PI) in MIA PaCa-2 cells. Cells were exposed to 125µg/ml, 250 µg/ml and 500 µg/ml of 0 mM, 30 mM and 60 mM NaCl-treated ethanol extracts of C*istus creticus*, respectively for 24 h (Scale bar = 100 µm).

In AsPC-1 cells, 0 mM and 30 mM NaCl-treated plant extracts showed similar effect on decreasing mitochondrial membrane potential at the 250 µg/ml and 500 µg/ml concentrations. 500 µg/ml of 60 mM NaCl-treated plant extract showed the most significant effect on decreasing the mitochondrial membrane potential. It was observed that mitochondrial membrane potential fluorescence signals were significantly decreased with the increasing concentrations of all salinity stress groups. The least effect on decreasing mitochondrial membrane potential was observed in 30 mM NaCl-treated plant extracts. PI fluorescence signals were increased with increasing concentrations for all salinity groups. Increasing number of death cells were observed with increasing concentrations of all salinity stress groups. 500 µg/ml of 0 mM and 60 mM NaCl-treated plant extract was the most effective on increasing the cell death by disrupting mitochondrial membrane potential which was shown in Figure 3.7.

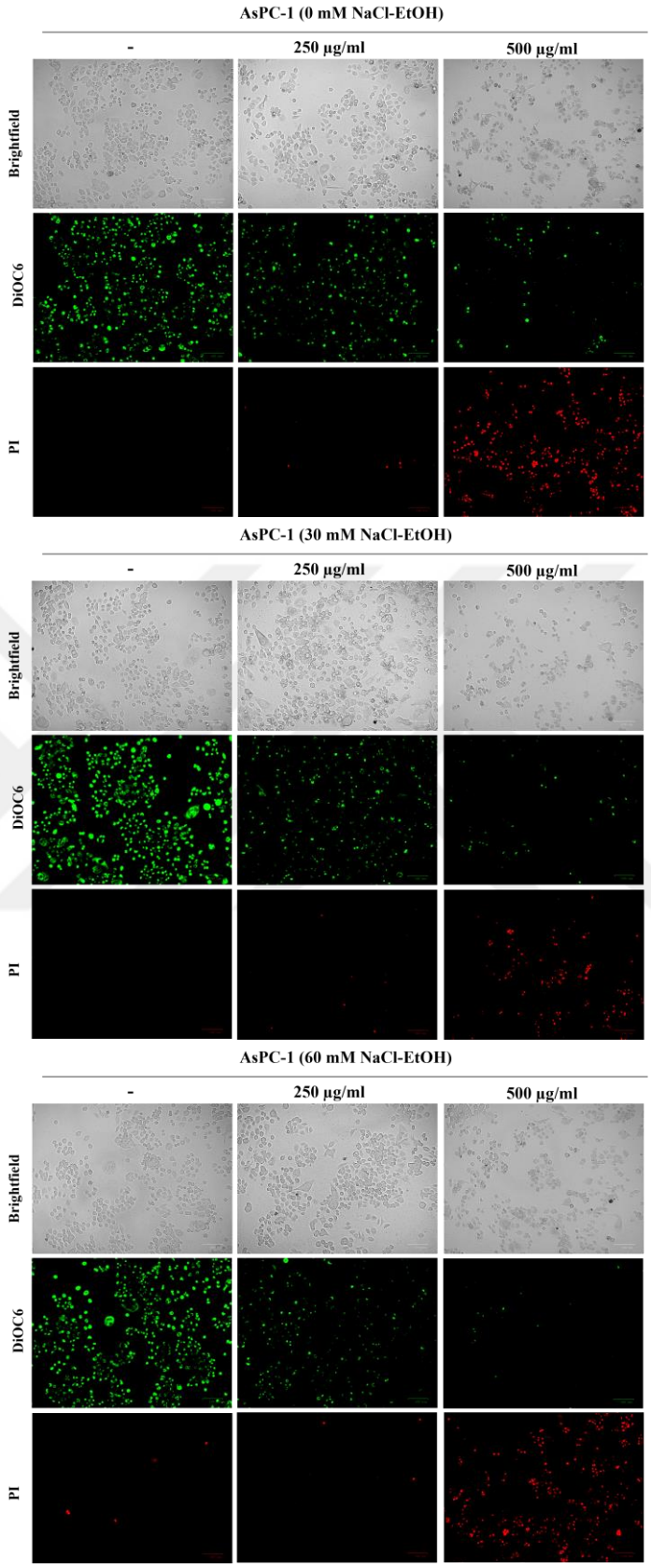

Figure 3.7. Fluorescence signals of mitochondria of live cells by DiOC6 (3,3'-Dihexyloxacarbocyanine Iodide) and DNA in apoptotic cells by Propidium Iodide (PI) in AsPC-1 cells. Cells were exposed to 125µg/ml, 250 µg/ml and 500 µg/ml of

0 mM, 30 mM and 60 mM NaCl-treated ethanol extracts of C*istus creticus*, respectively for 24 h (Scale bar = 100 μm).

As a result, due to 0 mM and 60 mM of NaCl-treated *C. creticus* extracts showed similar anti-cancer effects on pancreatic cancer cell lines, ethanol extracts of 30 mM and 60 mM NaCl-treated plants were selected for further experiments.

3.4. Increasing concentrations of ethanol extracts of *C. creticus* grown under different salinity stresses triggered formation of lipid droplets in pancreatic cancer cell lines.

Subcellular neutral lipid droplets by BODIPY as green color and DNA condensation in nucleus due to DNA breaks of cells by DAPI as blue color were detected in PANC-1, MIA PaCa-2 and AsPC-1 cells. Cells were exposed to 250 μg/ml and 500 μg/ml of 30 mM and 60 mM NaCl-treated *C. creticus* extracts through the EtOH extraction method for 24 h.

Considering the PANC-1 cells, lipid droplets were increased with the increasing concentrations of both 30 mM and 60 mM NaCl-treated plant extracts. The most effective increase in the number of small fragments of lipid droplets was observed in 500 μg/ml of 60 mM NaCl-treated plant extract treatment. The highest number of stained nuclear DNA of dead cells were observed by DAPI in 500 μg/ml of 60 mM NaCl-treated plant extract treatment. 500 μg/ml of 60 mM NaCl-treated ethanol extract of *C. creticus* showed the most effective result on inducing lipid-mediated cell death in PANC-1 cells which was shown in Figure 3.8.

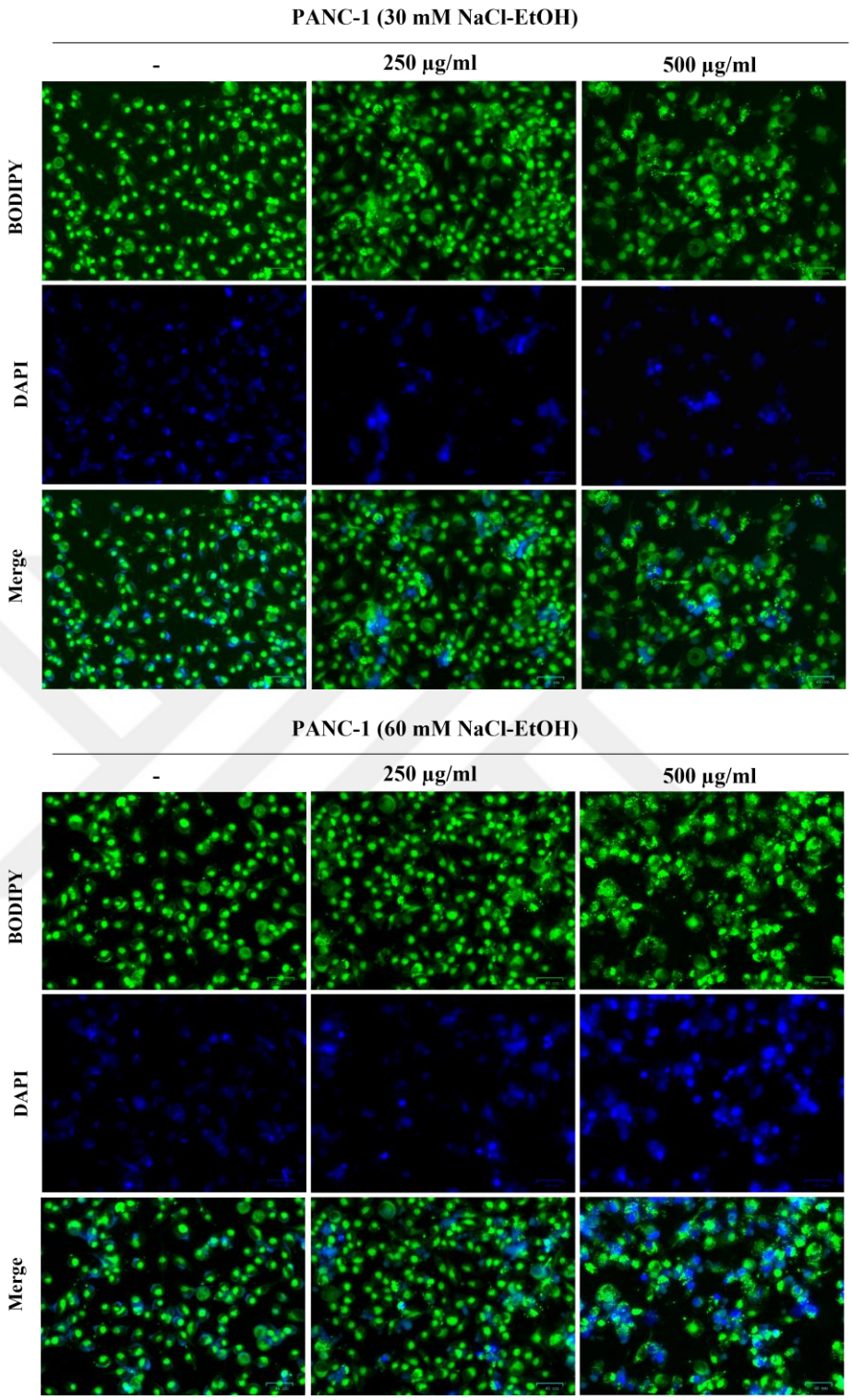

Figure 3.8. Fluorescence signals of lipid droplets by BODIPY® 493/503 and nucleus by DAPI in PANC-1 cells. Cells were exposed to 250 µg/ml and 500 µg/ml of 30 mM (a) and 60 mM (b) NaCl-treated C*istus creticus* extracts through ethanol extraction method for 24 h (Scale bar = 45 µm).

In MIA PaCa-2 cells, lipid droplets were increased with the increasing concentrations of both 30 mM and 60 mM NaCl-treated plant extracts. The most effective increase in the number of small fragments of lipid droplets was observed in 500 μg/ml of 60 mM NaCl-treated plant extract treatment. The highest number of stained nuclear DNA of dead cells were observed by DAPI in 500 μg/ml of 60 mM NaCl-treated plant extract treatment. 500 μg/ml of 60 mM NaCl-treated ethanol extract of *C. creticus* showed the most effective result on inducing lipid-mediated cell death in MIA PaCa-2 cells which was shown in Figure 3.9.

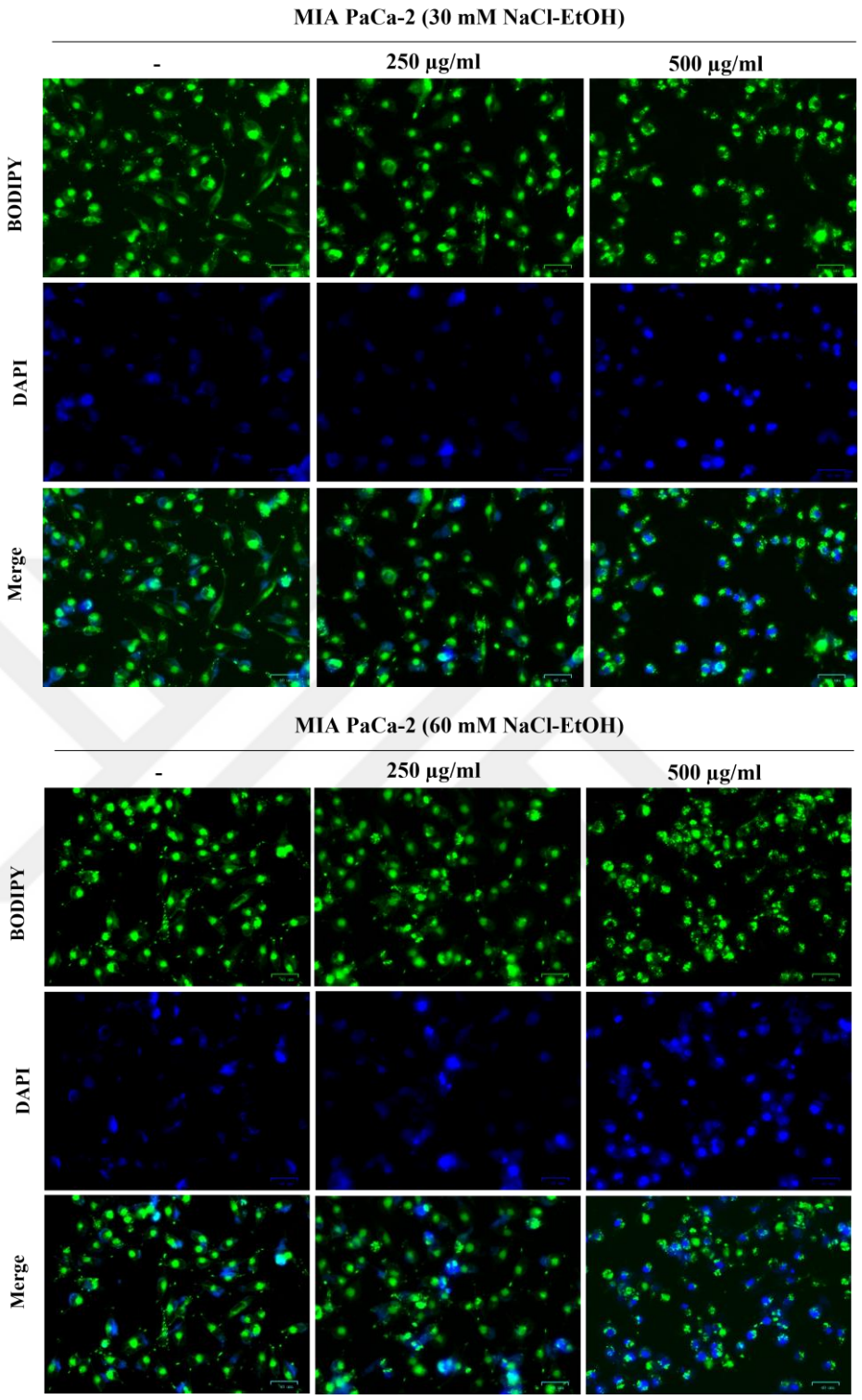

Figure 3.9. Fluorescence signals of lipid droplets by BODIPY® 493/503 and nucleus by DAPI in MIA PaCa-2 cells. Cells were exposed to 250 µg/ml and 500 µg/ml of 30 mM (a) and 60 mM (b) NaCl-treated C*istus creticus* extracts through ethanol extraction method for 24 h (Scale bar = 40 µm).

In AsPC-1 cells, the presence of lipid droplets did not change until the dose of 250 μg/ml of 30 mM NaCl-treated plant extract treatment. A slight presence of lipid droplets was observed at 250 μg/ml of 60 mM NaCl-treated plant extract treatment. A significant increase in neutral lipid droplets were observed in 500 μg/ml of 60 mM NaCl-treated plant extract treatment group in AsPC-1 cells. There was no observed significant change in DNA fragmentation in nucleus of dead cells compared to control group which was shown in Figure 3.10.

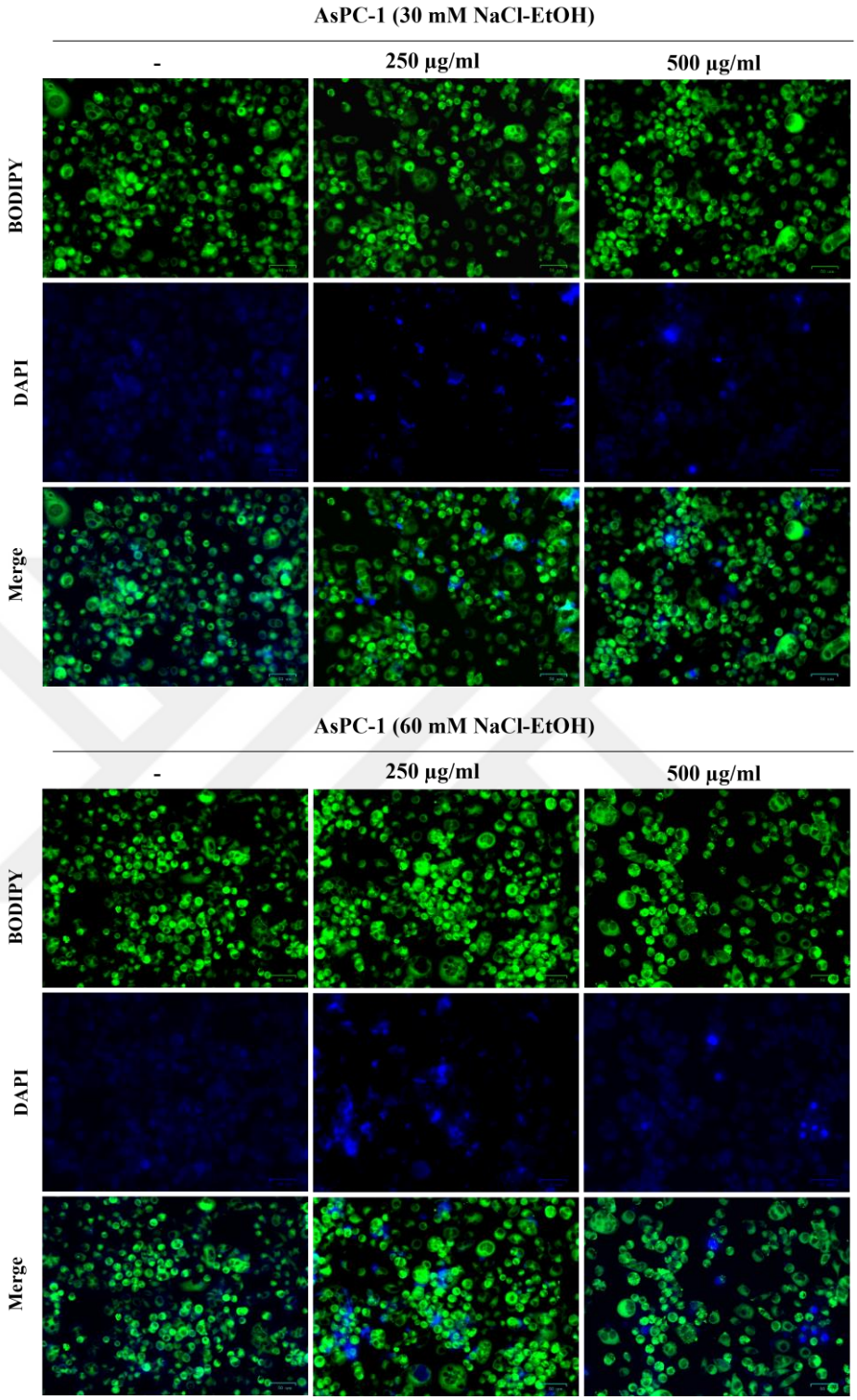

Figure 3.10. Fluorescence signals of lipid droplets by BODIPY® 493/503 and nucleus by DAPI in AsPC-1 cells. Cells were exposed to 250 µg/ml and 500 µg/ml of 30 mM and 60 mM NaCl-treated C*istus creticus* extracts, respectively through ethanol extraction method for 24 h (Scale bar = 50 µm).

Among all the cell lines, the cells that responded effectively to neutral lipid formation change and to staining the nuclei of dead cells were PANC-1 and MIA

PaCa-2 cells in response to 500 µg/ml of 60 mM NaCl-treated *C. creticus* to induce lipid-mediated cell death. AsPC-1 cells were the most resistant cells in response to *C. creticus* treatment. Therefore, 60 mM of 500 µg/ml of ethanol and water extracts were selected for further experiments to compare.

3.5. *C. creticus* induced lipid metabolism-mediated autophagy, apoptosis and necroptosis depending on extraction method.

PANC-1, MIA PaCa-2 and AsPC-1 cells were treated with a selected doses of 500 µg/ml EtOH extract and 500 µg/ml H_2O extract of 60 mM NaCl-treated *C. creticus* for 24 h and western blotting technique was performed to understand molecular mechanism of *C. creticus* on pancreatic cancer cell lines. Antibodies that are specific to necroptosis and autophagy signaling pathways were used for western blotting (Figure 3.11.)

Considering the PANC-1 cells, RIP levels were decreased slightly in 500 µg/ml EtOH and increased in 500 µg/ml H_2O treatment whereas MLKL levels were significantly decreased in both 500 µg/ml EtOH and 500 µg/ml H_2O treatment groups. A significant increase in PARP were observed in 500 µg/ml H_2O treatment groups compared to 500 µg/ml EtOH group. A slight decrease was observed in ATG7 levels regarding to 500 µg/ml EtOH treatment and similar expression levels were observed between control and 500 µg/ml H_2O treatment group. There was no significant difference between the expression levels of ATG16L1 between control and treatment groups. A slight downregulation in Beclin-1 levels was observed in 500 µg/ml EtOH whereas no difference was observed in 500 µg/ml H_2O treatment group. ATG5 expression levels between control group, 500 µg/ml EtOH and 500 µg/ml H_2O groups were also similar. A slight upregulation in ATG12 expression levels were observed in 500 µg/ml H_2O treatment group. The most significant upregulation in the expression levels of LC3A/B were observed in 500 µg/ml EtOH treatment group than 500 µg/ml H_2O compared to control group. B-actin was used as an internal control which was shown in Figure 3.11.

In MIA PaCa-2 cells, RIP levels were decreased slightly against 500 µg/ml EtOH and 500 µg/ml H_2O treatments. MLKL levels were significantly decreased in both 500 µg/ml EtOH and 500 µg/ml H_2O treatment groups. PARP levels were

upregulated against 500 µg/ml H_2O treatment groups compared to control and 500 µg/ml EtOH treatment group. A slight decrease was observed in ATG7 expression levels of both 500 µg/ml EtOH and 500 µg/ml H_2O treatment groups. More downregulation in 500 µg/ml EtOH group than 500 µg/ml H_2O was observed in ATG16L1 levels. There was no significant difference observed between 500 µg/ml EtOH and 500 µg/ml H_2O treatment group for Beclin-1 expression levels. No significant difference between control, 500 µg/ml EtOH and 500 µg/ml H_2O groups were observed regarding to ATG5 expression level. Downregulation in ATG12 expression levels were observed in both 500 µg/ml EtOH and 500 µg/ml H_2O treatment groups. There was more significant upregulation was observed in 500 µg/ml EtOH treatment group than 500 µg/ml H_2O compared to control group regarding the expression levels of LC3A/B. B-actin was used as an internal control which was shown in Figure 3.11.

Considering the AsPC-1 cells, RIP levels were slightly increased against 500 µg/ml EtOH compared to control and 500 µg/ml H_2O group. MLKL levels were significantly increased in 500 µg/ml EtOH than 500 µg/ml H_2O treatment groups compared to control group. PARP levels were downregulated against the 500 µg/ml EtOH, and 500 µg/ml H_2O treatment groups compared to control group. A slight increase was observed in ATG7 expression levels of both 500 µg/ml EtOH and 500 µg/ml H_2O treatment groups. ATG16L1 levels were slightly increased in both 500 µg/ml EtOH group and 500 µg/ml H_2O treatment groups. Beclin-1 expression levels were upregulated in 500 µg/ml EtOH group whereas the 500 µg/ml H_2O treatment group did show similar expression level with the control group. In a similar way, ATG5 expression levels were upregulated in 500 µg/ml EtOH group whereas the 500 µg/ml H_2O treatment group did show similar expression level with the control group. In LC3A/B expression, 500 µg/ml EtOH group was significantly upregulated than 500 µg/ml H_2O compared to control group. B-actin was used as an internal control which was shown in Figure 3.11.

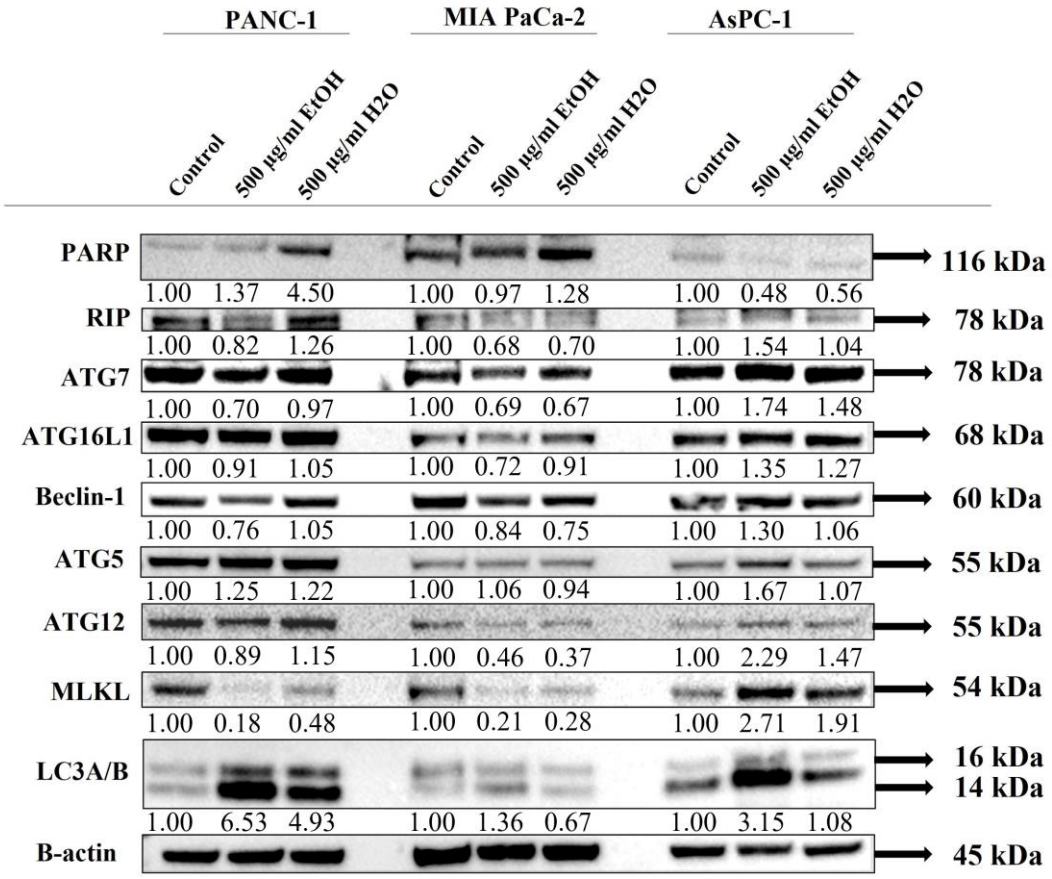

Figure 3.11. Effects of 60 mM NaCl-treated 500 µg/ml EtOH and 500 µg/ml H_2O extracts on pancreatic cancer cell lines for 24 h, and the protein expression levels of important molecular targets associated with autophagy, necroptosis and apoptosis by western blotting. β-actin was used as a loading control.

In the second part of western blotting, PANC-1, MIA PaCa-2 and AsPC-1 cells were treated with a selected doses of 500 µg/ml EtOH extract and 500 µg/ml H_2O extract of 60 mM NaCl-treated *C. creticus* for 24 h and western blotting technique was performed to understand molecular mechanism of *C. creticus* on pancreatic cancer cell lines. Antibodies that are specific to MTOR, fatty acid and lipid metabolism signaling pathways were used for western blotting (Figure 3.12.)

In PANC-1 cells in MTOR signaling pathway, Ras levels were increased against both 500 µg/ml EtOH and 500 µg/ml H_2O treatment groups. MTOR expression was slightly decreased in both 500 µg/ml EtOH and 500 µg/ml EtOH treatment group was more downregulated than 500 µg/ml H_2O compared to control group. A slight decrease in 500 µg/ml EtOH treatment group compared to control group was observed in Raptor levels whereas the 500 µg/ml H_2O treatment group did show similar expression level with the control group. AMPKα2 levels were

significantly decreased in 500 µg/ml EtOH treatment group whereas the expression level of AMPKα2 were increased in 500 µg/ml H_2O treatment group. Upregulation in Phospho-AMPKβ1 expression was observed in 500 µg/ml H_2O treatment group while Phospho-AMPKβ1 were downregulated in 500 µg/ml EtOH treatment group. RAGC levels were slightly increased in both treatment groups compared to control groups. LAMTOR1 levels were significantly decreased against 500 µg/ml EtOH treatment but there was no significant change observed between control and 500 µg/ml H_2O group (Figure 3.12.)

Considering the PANC-1 cells in fatty acid and lipid metabolism signaling pathway, upregulation in ACC expression was observed in both 500 µg/ml H_2O and 500 µg/ml EtOH, respectively. FASN expression levels were significantly increased in both 500 µg/ml EtOH and 500 µg/ml H_2O compared to control group. A significant increase in ATP-citrate lyase was observed against both 500 µg/ml EtOH and 500 µg/ml H_2O treatment groups. AceCS1 was upregulated in both treatment groups equally, compared to control group. There was no significant change observed in Fumarase expression against both treatment groups compared to control group. B-actin was used as an internal control which was shown in Figure 3.12.

In MIA PaCa-2 cells in MTOR signaling pathway, Ras levels were not changed against both 500 µg/ml EtOH and 500 µg/ml H_2O treatment groups compared to control group. MTOR expression was significantly decreased in 500 µg/ml EtOH whereas 500 µg/ml H_2O treatment did not change the MTOR expression level. A significant decrease in 500 µg/ml EtOH treatment group compared to control group was observed in Raptor levels. AMPKα2 levels were significantly decreased in 500 µg/ml EtOH and 500 µg/ml H_2O treatment group, respectively. Downregulation in phospho-AMPKβ1 expression was observed in both 500 µg/ml EtOH and 500 µg/ml H_2O treatment groups. RAGC levels were increased in both treatment groups compared to control groups. LAMTOR1 levels were significantly decreased against 500 µg/ml EtOH treatment and 500 µg/ml H_2O, respectively (Figure 3.12.)

Considering the MIA PaCa-2 cells in fatty acid and lipid metabolism signaling pathway, significant downregulation in ACC expression was observed in both 500 µg/ml EtOH and 500 µg/ml H_2O, respectively. FASN expression levels were significantly decreased in both 500 µg/ml EtOH and 500 µg/ml H_2O compared to

control group. A slight decrease in ATP-citrate lyase was observed against both 500 µg/ml EtOH and 500 µg/ml H_2O treatment groups. AceCS1 was downregulated in 500 µg/ml EtOH treatment group whereas no change was observed in 500 µg/ml H_2O treatment group compared to control group. There was a slight increase observed in Fumarase expression against both treatment groups compared to control group. B-actin was used as an internal control which was shown in Figure 3.12.

In AsPC-1 cells in MTOR signaling pathway, Ras levels were downregulated in 500 µg/ml EtOH and were upregulated in 500 µg/ml H_2O treatment group. MTOR expression level did not change significantly for both treatment groups. A significant decrease in 500 µg/ml EtOH treatment group compared to control group was observed in Raptor levels. AMPKα2 levels were decreased in 500 µg/ml EtOH and slightly increased in 500 µg/ml H_2O treatment group compared to control group. Downregulation in phospho-AMPKβ1 expression was observed in both 500 µg/ml EtOH and 500 µg/ml H_2O treatment groups, respectively. RAGC levels were not changed in both treatment groups compared to control groups. LAMTOR1 levels in both treatment groups were similarly upregulated (Figure 3.12.)

Considering the AsPC-1 cells in fatty acid and lipid metabolism signaling pathway, a slight downregulation in ACC expression was observed in both 500 µg/ml EtOH and 500 µg/ml H_2O, respectively. FASN expression levels were slightly decreased in both 500 µg/ml EtOH and 500 µg/ml H_2O compared to control group. A slight decrease in ATP-citrate lyase was observed in 500 µg/ml EtOH but there was no change observed in 500 µg/ml H_2O treatment group. AceCS1 was upregulated in both 500 µg/ml H_2O and 500 µg/ml EtOH treatment group, respectively. There was no significant change observed in Fumarase expression against both treatment groups compared to control group. B-actin was used as an internal control which was shown in Figure 3.12.

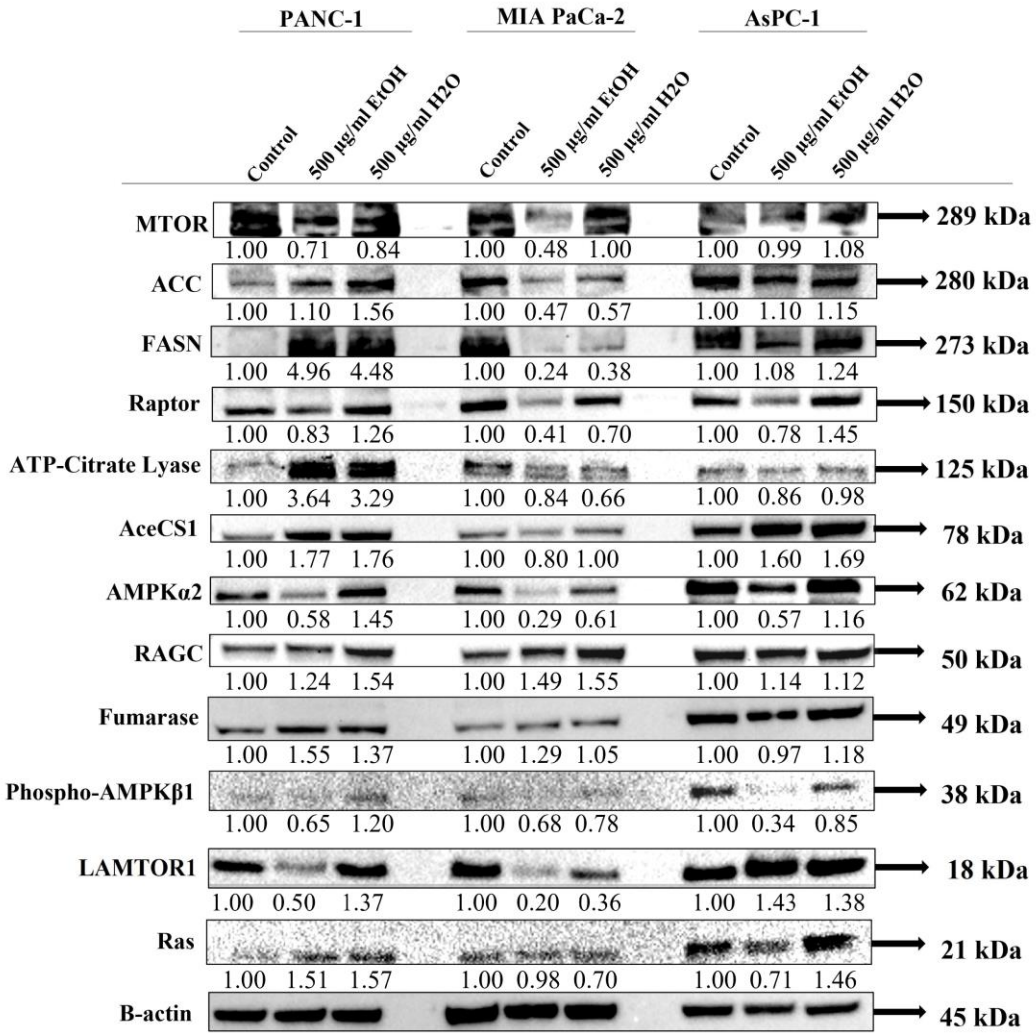

Figure 3.12. Effects of 60 mM NaCl-treated 500 μg/ml EtOH and 500 μg/ml H_2O extracts on pancreatic cancer cell lines for 24 h, and the protein expression levels of important molecular targets associated with fatty acid and lipid metabolism by western blotting. β-actin was used as a loading control.

4. DISCUSSION and CONCLUSION

In recent years, the incidence and mortality rate of pancreatic cancer have both increased among the population globally. It is slightly more common in men than women, although the frequency has become nearly equal in recently. Age, gender, smoking, prolonged alcohol use, family history, chronic pancreatitis, previous exposure to abdominal radiation, and the increase in obesity are some of the risk factors that contribute to cancer. The primary method of treating pancreatic cancer is surgical excision of the tumor, which is generally followed by chemotherapy and radiation therapy. However, in instances of locally advanced disease, tumor shrinking and inhibition via chemoradiotherapy can improve the success of surgery. However, early diagnosis and treatment of pancreatic cancer are challenging due to its limited therapeutic options, and the disease exhibits resistance to conventional treatment methods, often due to specific mutations such as KRAS, SMAD, TP53, CDK2NA, which contribute to an aggressive disease profile [59]. As a result, presence of these mutations in pancreatic cancer cells has a negative impact on the effectiveness of medications, highlighting the requirement for the creation of new therapeutic models or combined therapy models to overcome with these challenges.

Naturally derived compounds potentially provide fewer toxic effects than existing treatments such as chemotherapy. These compounds are produced from plants, and they include important bioactive which exert promising anti-cancer properties to develop clinical drugs are currently being studied. So far, it has been found that plant-derived compounds exhibit the inhibition of tumor growth and trigger cell death [60]. Moreover, a variety of abiotic stresses on plants including drought, salinity, extreme temperatures restrict the growth and productivity of plants. Especially, salinity (salt) stress is one of the most significant stress factors restricting plant growth and development and has a negative impact on a variety of physiological and biochemical processes for the plant itself. The development and production of therapeutic and aromatic plants are closely correlated with changes in cultivation practices and external environmental conditions, which in turn affect the metabolic pathways that lead to the accumulation of natural compounds. Additionally, salt stress is a key element that adversely affects plant growth and the production of antioxidant elements, secondary metabolites and increase in

polyphenol content [61]. In this study, anti-cancer and therapeutic effects of ethanol and distilled water isolates of *Cistus creticus* L., which is grown under 0 mM, 30 mM, and 60 mM NaCl concentrations, on PANC-1, MIA PaCa-2 and AsPC-1 cell lines were evaluated.

Measurement of cellular metabolic activity was a first step, and it is crucial to determine cell viability and cytotoxicity effect of *C. creticus* treatments on pancreatic cancer cell lines. The MTT can pass through the membrane of viable cells and the inner membrane of mitochondria to undergo reduction. This reduction disrupts the core tetrazole ring of MTT and forms formazan crystals, a violet-blue water-insoluble molecule by living cells [62]. Cytotoxic responses against three different concentrations (125 μg/ml, 250 μg/ml and 500 μg/ml) of each three different salt concentrations of *C. creticus* extracts (0, 30, 60 mM of NaCl) through EtOH and water extraction method for 24 h on PANC-1, MIA PaCa-2 and AsPC1 cells were evaluated. As a result, ethanol extracts of *C. creticus* had the most effective cytotoxicity inhibition in every concentration of NaCl-treated plants than distilled water extracts according to Figure 3.1. The most common effective inhibition was observed in 0 mM and 60 mM NaCl-treated *C. creticus* plants for all cell lines. The most effective cytotoxicity was observed after 250 μg/ml dosage for ethanol groups. Thus, *C. creticus* extracts dissolved in ethanol had a more significant effect in cell viability. It can be concluded that ethanol is a better solvent than water to protect and increase the efficiency of the chemical composition of the phenolic content of the plant. Also, the cell viability of pancreatic cancer cells decreased with the increasing concentrations of plant extracts and the increasing concentration of salinity stress. So, increased total phenolic content of *C. creticus* has a significant therapeutic effect on cells. Cells were relatively resistant to dose of 125 μg/ml of plant extracts. Interestingly, there was a sudden decrease in relative cell viability between the concentrations of 250 μg/ml and 500 μg/ml of plant extracts which might be considered a therapeutic dose range. However, the cell viability was increased in AsPC-1 cells at concentrations of 125 μg/ml and 250 μg/ml for both EtOH and water-extracted *C. creticus* treatments. In addition, AsPC1 cells were more sensitive than other cell lines at the concentration of 500 μg/ml extract treatment (Figure 3.1.). The genetic characterization of AsPC-1 cells might cause this difference because AsPC1 cells were derived from nude mode xenograft that form from ascites and

AsPC-1 cell line derived xenograft (CDX) model from metastatic tissues induce the suppression of innate immune system whereas PANC-1 and MIA PaCa-2 cells were derived from primary pancreatic tumor and activate innate immune responses [63].

Colony formation abilities of pancreatic cancer cells from a single cell were also investigated. Colony formation assay is a vital experiment to evaluate the survival and reproduction ability of a single cell to form colonies against a cytotoxic agent. In this study, Pancreatic cancer cells were exposed to increasing concentrations of ethanol and water extracts (50, 100, 150, 250 and 500 μg/ml of 60 mM NaCl-treated *C. creticus)* for 24 h. It is demonstrated that the lower concentrations (0-50 μg/ml) of water-extracted *C. creticus* have increased colony-forming ability in PDAC cells whereas EtOH extract had linear decreasing activity on colony formation. A significant decrease in colony-forming ability was observed after 100 μg/ml of EtOH extracts whereas a significant decrease in colony-forming ability was observed after 150 μg/ml of water extracts (Figure 3.2.). These results showed a positive correlation with the previous MTT assay experiment. Lower doses of *C. creticus* water extracts showed inducing effects on colony forming ability of cancer cell. This might result in a specific cut-off value of pharmacological composition and effectiveness of *C. creticus*.

Intracellular ROS levels were also studied by spectrophotometric detection using CM-H2DCFDA dye. Hydrogen peroxide (H2O2), superoxide (O2•-), and the hydroxyl radical (•OH) are examples of well-known ROS. Biomolecules like lipids, proteins and DNA may become oxidatively damaged as a result of excessive ROS generation. Reactive oxygen species (ROS) are highly reactive byproducts of normal metabolic processes of cells by mitochondria [64]. These byproducts can serve as secondary messengers in cell signaling for both normal and cancer cells. ROS levels are generally elevated in tumor cells due to increased metabolism, and gene mutation and ROS levels can be suppressed by antioxidant therapy in tumor cells. In this study, the increased total antioxidant capacity of EtOH-extracted *C. creticus* with the increasing salinity stress decreased intracellular ROS levels in PDAC cell lines (Figure 3.2.). Non-treated cancer cells showed the highest ROS levels. In contrast, EtOH-extracted plants exposed to the highest salinity stress has significantly eliminated ROS levels. Therefore, increased antioxidant capacity with the increasing salinity stress of *C. creticus* has a potential therapeutic effect of decreasing ROS

levels in pancreatic cancer cell lines. Interestingly, Reactive oxygen species (ROS) appear to play a dual role in cancer cells, according to mounting scientific evidence. For cancer cell homeostasis and the proper execution of cellular events such proliferation, differentiation, migration, and programmed cell death, maintaining a sufficient level of ROS is crucial. Elevated ROS levels have a negative impact on cancer cells, ultimately causing their mortality. However, ROS levels were decreased against *C. creticus* treatment and support cell death. This might be result from strong antioxidant capacity of *C. creticus* due to antioxidants are capable of scavenging ROS, hence lowering oxidative stress. They are well known for their therapeutic effects in the prevention and treatment of cancer [65]. According to a study, deferasirox (DFX), which is an oral iron chelator, induces apoptosis in multiple myeloma (MM) cells via inhibiting intracellular ROS [66]. In addition, disrupted mitochondria in PDAC cells might lead to decreased ROS level due to ROS are mainly synthesized from mitochondria.

Mitochondrial changes by MitoTracker Red CMXRos fluorescence signals in pancreatic cancer cells were also investigated. Cells were exposed to three different concentrations (125 μg/ml, 250 μg/ml and 500 μg/ml) of each three different salt concentrations of *C. creticus* extracts (0, 30, 60 mM of NaCl) through the EtOH and water extraction method for 24 h. As a result, EtOH extract treatment was more effective than water extract treatment in PDAC cells. The most significant decrease in mitochondrial activity and function depending on membrane potential was observed in MIA PaCa-2 and AsPC-1 cells with a concentration of 250 μg/ml, respectively in EtOH extraction. 30 mM NaCl-treated plant had the least effect on decreasing mitochondrial activity among other experimental groups and 0 mM, and 60 mM NaCl-treated *C. creticus* plant extracts showed similar effects on decreased mitochondrial membrane potential (Figure 3.4.). This might be result from 30 mM NaCl is an optimum plant cultivation nutrient condition to provide adequate level of minerals for healthy plant growth whereas both inadequate 0 mM (no salt) and excessive 60 mM (high salt) nutrient conditions might lead abiotic stress for *C. creticus* which alter secondary metabolites and antioxidant levels. It can also be concluded that the antioxidant capacity of *C. creticus* under salinity stress can be used as a promising mitochondria-targeted antioxidant therapy for pancreatic cancer.

Based on previous data, EtOH extracts were chosen for fluorescent staining experiments. Changes in mitochondrial membrane potential by DiOC6 and dead cells of DNA in nucleus by propidium iodide (PI) were performed on PDAC cell lines. Cells were exposed to 250 μg/ml and 500 μg/ml of each three different salt concentrations of *C. creticus* extracts (0, 30, 60 mM of NaCl) through the EtOH extraction method for 24 h. PI was used to stain dead cells whereas DiOC6 was used to stain cells that have active mitochondrial membrane potential as an indicator of increased metabolism. As a result, increasing number of dead cells were observed with increasing concentrations of all salinity stress groups in all PDAC cells (Figure 3.5., Figure 3.6., Figure 3.7.). The most significant therapeutic effect was observed in 500 μg/ml of 60 mM EtOH extracts which showed positive correlation with MitoTracker data. It can be concluded that *C. creticus* is targeting mitochondria and disrupts cell metabolism.

Neutral lipid droplets by BODIPY and DNA condensation by DAPI were performed and PDAC cells were exposed to 250 μg/ml and 500 μg/ml of 30 mM and 60 mM NaCl-treated *C. creticus* extracts through the EtOH extraction method for 24 h. The dynamic organelles known as lipid droplets are made up of neutral lipids, triacylglycerides (TAG) and cholesterol esters which are encased by a monolayer of and connected proteins. They are included in cellular processes such as regulating energy, storing fatty acids, signaling with lipids, and mediating toxicity with lipids. Lipid droplets also participate in apoptotic processes through interacting with the endoplasmic reticulum and mitochondria [67]. The most effective increase in the number of neutral lipid droplets was observed in 500 μg/ml of 60 mM NaCl-treated plant extract treatment on MIA PaCa-2 and PANC-1, respectively whereas AsPC-1 cells were the most resistant cells in response to *C. creticus* treatment (Figure 3.8., Figure 3.9., Figure 3.10.). The formation of lipid droplets that were visualized by BODIPY also might result from apoptotic bodies leading cell death. Due to metastatic nature of AsPC-1 might be the reason of its resistance to treatment. DAPI dye was used to dye adenine and tyrosine rich sites of condensed DNA due to apoptosis and in order to DAPI to enter the cell, cells must permeabilized [68]. According to this information, cells that have disrupted membrane due to the *C. creticus* treatment were stained and visualized by DAPI. Among all the cell lines, the cells that responded effectively to neutral lipid droplet formation and to staining the

nuclei of dead cells were PANC-1 and MIA PaCa-2 cells in response to 500 μg/ml of 60 mM NaCl-treated *C. creticus* to induce lipid-mediated cell death which was supported by merging two fluorescence stain (Figure 3.8., Figure 3.9.). AsPC-1 cells were the most resistant cells in response to *C. creticus* treatment for this experiment which was validated and showed positive correlation with previous data (Figure 3.10.).

This study also evaluated the molecular mechanisms of autophagy, apoptosis and necroptosis signaling cascades of PDAC cells against 500 μg /ml to compare EtOH extraction and water extraction methods of 60 mM NaCl-treated *C. creticus*. Considering autophagy, ATG5 and ATG12 conjugate and interact noncovalently with Autophagy Related 16 Like 1 (ATG16L1) to form a large complex through Autophagy Related 7 (ATG7) with Beclin-1. This complex induces autophagosome formation with ATG7 and ATG3 (E1 and E2-like enzymes), and LC3A/B executes LC3 lipidation and autophagy sequestration [48]. The expression of ATG5 was significantly increased with 500 μg /ml EtOH-extracted plant treatment for all PDAC cells (Figure 3.11). This validates *C. creticus* treatment has a potential effect on inducing autophagy. There was also a significant increase in the expression of ATG16L1 for PANC-1 and AsPC-1 cells concerning plant extracts treatment. Interestingly, there was a significant decrease in ATG12 expression in MIA PaCa-2 cells concerning plant treatment. This might result from another decreased expression level of ATG16L1 protein in MIA PaCa-2 cells. Induced autophagy was also validated by a remarkable increase in the expression of LC3A/B protein in all PDAC cell lines due to *C. creticus* therapeutic. This study also investigated necroptosis by evaluating MLKL and RIP biomarkers to enlighten the crosstalk between cell death and cell survival modalities. Necroptosis is a regulated necrosis RIP kinase-dependent necrotic cell death when RIP is phosphorylated. RIP recruits and phosphorylated MLKL to form complex II c necrosome. After phosphorylation, MLKL oligomerizes and causes membrane rupture and cell death [50]. According to results, MLKL and RIP were decreased in both PANC-1 and MIA PaCa-2 cells, whereas there was a significant increase in necroptosis in AsPC-1 cells. This difference between cell lines might result from a mutation profile among cell lines (Figure 3.11.). PARP is an enzyme found in the nucleus activated by DNA strand breaks during apoptosis. Excessive activation of PARP can lead to necrotic and

apoptotic cell death [50]. According to protein expression levels in Figure 3.11., PARP expression levels were increased in PANC-1, and MIA PaCa-2 cells whereas PARP expression levels were decreased in AsPC-1 cells. This difference with increased MLKL levels in AsPC-1 cells might indicate that AsPC-1 might tend to undergo necroptosis than apoptosis when exposed to *C. creticus* extracts.

In this thesis, lipid metabolism was also investigated to understand crosstalk between cell death by western blotting. According to Figure 3.12, mTOR and Raptor levels were downregulated in EtOH extracted plant treatment in all the PDAC cells while AMPK α and p-AMPKβ1 was also inhibited in EtOH group for all PDAC cells. Interestingly, RAPTOR is phosphorylated by AMPK results in inhibition of mTOR [42]. However, both AMPK, Raptor and MTOR were downregulated against EtOH group treatment. This might be the result from mTOR inhibition was occurred independent of AMPK expression. ACC, FASN, AceCS1 levels were upregulated in PANC-1 and AsPC-1 cells in EtOH group whereas they were inhibited in MIA PaCa-2 cells. According to the literature, inhibition of mTOR upregulates ACC, FASN and AceCS1 protein in lipid metabolism [69]. However, MIA PaCa-2 cells showed decreasing expression level of these proteins in EtOH group. This might be the result from involvement or different genetic mutation profile. ATP-citrate lyase was significantly upregulated in PANC-1 cells whereas a slight decrease occurred in MIA PaCa-2 and AsPC-1 cells in EtOH group. The reason might be the similar overexpression of FASN in PANC-1 and a strong link between ATP-citrate lyase protein that indicates strong response against antioxidant treatment by *C. creticus.* There was also an increase in Fumarase observed in PANC-1 cells rather than MIA PaCa-2 and AsPC-1. The reversible hydration of fumarate to malate is catalyzed by the fumarase which is a member of the tricarboxylic acid cycle (TCA) and generates reducing equivalents to support oxidative ATP production that is important for cellular energetics system occurs in mitochondria [70]. Reduced mitochondria activity with EtOH extract of *C. creticus* might trigger cellular response against stress. Additionally, decrease in AMPK might be the result from decreased Fumarase because Fumarase supports ATP production whereas AMPK expression increases in ATP decreased conditions. The relationship between AMPK and fumarase can be enlightened from opposite changes in expression profiles. There was a slight increase observed in EtOH group treatment for all PDAC cell lines. RAGC is GTPase which

regulates activity of mTOR activity and becomes active when it is GDP-bound RAGC and the increase in RAGC was observed in both EtOH and water groups for all PDAC cells. The RAGC might be present in its inactive form due to decrease in mTOR, because active RAGC binds to activate mTOR [71]. There was a significant decrease was observed in EtOH group of PANC-1 and MIA PaCa-2 cells whereas an increase was observed in EtOH group of AsPC-1 cells. Decreased level of LAMTOR1 might be related to inhibition of mTOR due to LAMTOR 1 belonging to the regulator complex and it is important to regulation of mTOR on lysosome with its binding with RAGC and serves as scaffold protein for mTORC1 [72]. In the absence of mTOR and LAMTOR1, RAGC might be present freely within cell due to its increased expression.

In overall, anti-cancer effects of 500 μg/ml of 0 mM and 60 mM NaCl-treated *C. creticus* showed better therapeutic effect on PDAC cell lines. PANC-1 and MIA PaCa-2 cells were more prone to undergo autophagy than necrosis with decreased MLKL levels, whereas AsPC-1 cells were more prone to undergo necroptosis than autophagy. It is also concluded that lipid metabolism was primarily affected by Cistus treatment because it was shown that it targeted activity of mitochondria independent from AMPK expression and ROS levels.

As a result, *C. creticus* extracts can be used as therapeutic agents and the solvent which is used for extraction has a critical role in the effectiveness of this natural compound. *C. creticus* is an effective and promising natural source of antioxidants and can play a significant role in cancer prevention and treatment. Future studies might also be critical to investigate the relationship between extraction methods, different stress factors and the therapeutic effectiveness of medicinal plants and the therapeutic effectiveness of herbs on cancer at molecular levels concerning the chemical composition of *C. creticus.* In future, the unusual relation between these compounds may provide a more comprehensive perspective on cancer research and medicinal plants by this thesis. Moreover, the importance of personalized medicine is highlighted by this research because even the cancer is developed from the same organ, many genetic alterations and mutations affect the anticancer impact and of any therapeutic agent.

REFERENCES

[1] Bardeesy, N., & DePinho, R. A., (2002), "Pancreatic cancer biology and genetics". Nature reviews, Cancer, 2(12), 897–909.

[2] Hu, J. X., Zhao, C. F., Chen, W. B., Liu, Q. C., Li, Q. W., Lin, Y. Y., & Gao, F., (2021), "Pancreatic cancer: A review of epidemiology, trend, and risk factors", World journal of gastroenterology, 27(27), 4298–4321.

[3] Collisson, E. A., Bailey, P., Chang, D. K., & Biankin, A. V., (2019), "Molecular subtypes of pancreatic cancer", Nature reviews, Gastroenterology & hepatology, 16(4), 207–220.

[4] Web 1, (2023), https://gco.iarc.fr, (Accessed on 28th June 2023).

[5] Midha, S., Chawla, S., & Garg, P. K., (2016), "Modifiable and non-modifiable risk factors for pancreatic cancer: A review", Cancer letters, 381(1), 269–277.

[6] Zhao, Z., & Liu, W., (2020), "Pancreatic Cancer: A Review of Risk Factors, Diagnosis, and Treatment", Technology in cancer research & treatment, 19, 1533033820962117.

[7] McGuigan, A., Kelly, P., Turkington, R. C., Jones, C., Coleman, H. G., & McCain, R. S., (2018), "Pancreatic cancer: A review of clinical diagnosis, epidemiology, treatment and outcomes" World journal of gastroenterology, 24(43), 4846–4861.

[8] Swidnicka-Siergiejko, A. K., Gomez-Chou, S. B., Cruz-Monserrate, Z., Deng, D., Liu, Y., Huang, H., Ji, B., Azizian, N., Daniluk, J., Lu, W., Wang, H., Maitra, A., & Logsdon, C. D., (2017), "Chronic inflammation initiates multiple forms of K-Ras-independent mouse pancreatic cancer in the absence of TP53", Oncogene, 36(22), 3149–3158.

[9] Garrido-Laguna, I., & Hidalgo, M., (2015), "Pancreatic cancer: from state-of-the-art treatments to promising novel therapies", Nature reviews, Clinical oncology, 12(6), 319–334.

[10] Demir, I. E., Jäger, C., Schlitter, A. M., Konukiewitz, B., Stecher, L., Schorn, S., Tieftrunk, E., Scheufele, F., Calavrezos, L., Schirren, R., Esposito, I., Weichert, W., Friess, H., & Ceyhan, G. O., (2018), "R0 Versus R1 Resection Matters after Pancreaticoduodenectomy, and Less after Distal or Total Pancreatectomy for Pancreatic Cancer", Annals of surgery, 268(6), 1058–1068.

[11] Wood, L. D., Canto, M. I., Jaffee, E. M., & Simeone, D. M., (2022), "Pancreatic Cancer: Pathogenesis, Screening, Diagnosis, and Treatment", Gastroenterology, 163(2), 386–402.e1.

[12] Springfeld, C., Jäger, D., Büchler, M. W., Strobel, O., Hackert, T., Palmer, D. H., & Neoptolemos, J. P., (2019), "Chemotherapy for pancreatic cancer", 48(3 Pt 2), e159–e174.

[13] Kolbeinsson, H. M., Chandana, S., Wright, G. P., & Chung, M., (2023), "Pancreatic Cancer: A Review of Current Treatment and Novel Therapies", 36(1), 2129884.

[14] Chin V, Nagrial A, Sjoquist K,. (2018), "Chemotherapy and radiotherapy for advanced pancreatic cancer", Cochrane Database Syst Rev. 28(18): 1875-2033.

[15] Wong, W., Raufi, A. G., Safyan, R. A., Bates, S. E., & Manji, G. A., (2020), "BRCA Mutations in Pancreas Cancer: Spectrum, Current Management, Challenges and Future Prospects", Cancer management and research, 12, 2731–2742.

[16] Buscail, L., Bournet, B., & Cordelier, P., (2020), "Role of oncogenic KRAS in the diagnosis, prognosis and treatment of pancreatic cancer", Nature reviews, Gastroenterology & hepatology, 17(3), 153–168.

[17] Janes, M. R., Zhang, J., Li, L. S., Hansen, R., Peters, U., Guo, X., Chen, Y., Babbar, A., Firdaus, S. J., Darjania, L., Feng, J., Chen, J. H., Li, S., Li, S., Long, Y. O., Thach, C., Liu, Y., Zarieh, A., Ely, T., Kucharski, J. M., Liu, Y., (2018), "Targeting KRAS Mutant Cancers with a Covalent G12C-Specific Inhibitor", Cell, 172(3), 578–589.e17.

[18] Ferri-Borgogno, S., Barui, S., McGee, A. M., Griffiths, T., Singh, P. K., Piett, C. G., Ghosh, B., Bhattacharyya, S., Singhi, A., Pradhan, K., Verma, A., Nagel, Z., Maitra, A., & Gupta, S., (2020), "Paradoxical Role of AT-rich Interactive Domain 1A in Restraining Pancreatic Carcinogenesis", Cancers, 12(9), 2695.

[19] Park, Y., Chui, M. H., Suryo Rahmanto, Y., Yu, Z. C., Shamanna, R. A., Bellani, M. A., Gaillard, S., Ayhan, A., Viswanathan, A., Seidman, M. M., Franco, S., Leung, A. K. L., Bohr, V. A., Shih, I. M., & Wang, T. L., (2019), "Loss of ARID1A in Tumor Cells Renders Selective Vulnerability to Combined Ionizing Radiation and PARP Inhibitor Therapy", Clinical cancer research : an official journal of the American Association for Cancer Research, 25(18), 5584–5594.

[20] Christenson, E. S., Jaffee, E., & Azad, N. S., (2020), "Current and emerging therapies for patients with advanced pancreatic ductal adenocarcinoma: a bright future", The Lancet. Oncology, 21(3), e135–e145.

[21] Lyssiotis, C. A., & Kimmelman, A. C., (2017), "Metabolic Interactions in the Tumor Microenvironment", Trends in cell biology, 27(11), 863–875.

[22] Halbrook, C. J., & Lyssiotis, C. A., (2017), "Employing Metabolism to Improve the Diagnosis and Treatment of Pancreatic Cancer", Cancer cell, 31(1), 5–19.

[23] Koppenol, W. H., Bounds, P. L., & Dang, C. V., (2011), "Otto Warburg's contributions to current concepts of cancer metabolism", Nature reviews. Cancer, 11(5), 325–337.

[24] Liberti, M. V., & Locasale, J. W., (2016), "The Warburg Effect: How Does it Benefit Cancer Cells?", Trends in biochemical sciences, 41(3), 211–218.

[25] Mayers, J. R., Torrence, M. E., Danai, L. V., Papagiannakopoulos, T., Davidson, S. M., Bauer, M. R., Lau, A. N., Ji, B. W., Dixit, P. D., Hosios, A. M., Muir, A., Chin, C. R., Freinkman, E., Jacks, T., Wolpin, B. M., Vitkup, D., & Vander Heiden, M. G., (2016), "Tissue of origin dictates branched-chain amino acid metabolism in mutant Kras-driven cancers", Science, 353(6304), 1161–1165.

[26] Li, X., Jiang, Y., Meisenhelder, J., Yang, W., Hawke, D. H., Zheng, Y., Xia, Y., Aldape, K., He, J., Hunter, T., Wang, L., & Lu, Z., (2016), "Mitochondria-Translocated PGK1 Functions as a Protein Kinase to Coordinate Glycolysis and the TCA Cycle in Tumorigenesis", Molecular cell, 61(5), 705–719.

[27] Nagarajan, A., Dogra, S. K., Sun, L., Gandotra, N., Ho, T., Cai, G., Cline, G., Kumar, P., Cowles, R. A., & Wajapeyee, N., (2017), "Paraoxonase 2 Facilitates Pancreatic Cancer Growth and Metastasis by Stimulating GLUT1-Mediated Glucose Transport", Molecular cell, 67(4), 685–701.e6.

[28] Zhang, C., Liu, J., Liang, Y., Wu, R., Zhao, Y., Hong, X., Lin, M., Yu, H., Liu, L., Levine, A. J., Hu, W., & Feng, Z., (2013), "Tumour-associated mutant p53 drives the Warburg effect", Nature communications, 4, 2935.

[29] Son, J., Lyssiotis, C. A., Ying, H., Wang, X., Hua, S., Ligorio, M., Perera, R. M., Ferrone, C. R., Mullarky, E., Shyh-Chang, N., Kang, Y., Fleming, J. B., Bardeesy, N., Asara, J. M., Haigis, M. C., DePinho, R. A., Cantley, L. C., & Kimmelman, A. C., (2013), "Glutamine supports pancreatic cancer growth through a KRAS-regulated metabolic pathway", Nature, 496(7443), 101–105.

[30] Abrego, J., Gunda, V., Vernucci, E., Shukla, S. K., King, R. J., Dasgupta, A., Goode, G., Murthy, D., Yu, F., & Singh, P. K., (2017), "GOT1-mediated anaplerotic glutamine metabolism regulates chronic acidosis stress in pancreatic cancer cells.", Cancer letters, 400, 37–46.

[31] Zaytouni, T., Tsai, P. Y., Hitchcock, D. S., DuBois, C. D., Freinkman, E., Lin, L., Morales-Oyarvide, V., Lenehan, P. J., Wolpin, B. M., Mino-Kenudson, M., Torres, E. M., Stylopoulos, N., Clish, C. B., & Kalaany, N. Y., (2017), "Critical role for arginase 2 in obesity-associated pancreatic cancer", Nature communications, 8(1), 242.

[32] Qin, C., Yang, G., Yang, J., Ren, B., Wang, H., Chen, G., Zhao, F., You, L., Wang, W., & Zhao, Y., (2020), "Metabolism of pancreatic cancer: paving the way to better anticancer strategies", Molecular cancer, 19(1), 50.

[33] Swierczynski, J., Hebanowska, A., & Sledzinski, T., (2014, "Role of abnormal lipid metabolism in development, progression, diagnosis and therapy of pancreatic cancer", World journal of gastroenterology, 20(9), 2279–2303.

[34] Currie, E., Schulze, A., Zechner, R., Walther, T. C., & Farese, R. V., (2013), "Cellular fatty acid metabolism and cancer", Cell metabolism, 18(2), 153–161.

[35] Ardito, C. M., Grüner, B. M., Takeuchi, K. K., Lubeseder-Martellato, C., Teichmann, N., Mazur, P. K., Delgiorno, K. E., Carpenter, E. S., Halbrook, C. J., Hall, J. C., Pal, D., Briel, T., Herner, A., Trajkovic-Arsic, M., Sipos, B., Liou, G. Y., Storz, P., Murray, N. R., Threadgill, D. W., Sibilia, M., Siveke, J. T., (2012), "EGF receptor is required for KRAS-induced pancreatic tumorigenesis", Cancer cell, 22(3), 304–317.

[36] Ricoult, S. J., Yecies, J. L., Ben-Sahra, I., & Manning, B. D., (2016), "Oncogenic PI3K and K-Ras stimulate de novo lipid synthesis through mTORC1 and SREBP", Oncogene, 35(10), 1250–1260.

[37] Porstmann, T., Santos, C. R., Griffiths, B., Cully, M., Wu, M., Leevers, S., Griffiths, J. R., Chung, Y. L., & Schulze, A., (2008) "SREBP activity is regulated by mTORC1 and contributes to Akt-dependent cell growth", Cell metabolism, 8(3), 224–236.

[38] Peterson, T. R., Sengupta, S. S., Harris, T. E., Carmack, A. E., Kang, S. A., Balderas, E., Guertin, D. A., Madden, K. L., Carpenter, A. E., Finck, B. N., & Sabatini, D. M., (2011), "mTOR complex 1 regulates lipin 1 localization to control the SREBP pathway", Cell, 146(3), 408–420.

[39] Koundouros, N., & Poulogiannis, G., (2020), "Reprogramming of fatty acid metabolism in cancer", British journal of cancer, 122(1), 4–22.
[40] Laplante, M., & Sabatini, D. M., (2009), "mTOR signaling at a glance", Journal of cell science, 122(Pt 20), 3589–3594.

[41] Toyama, E. Q., Herzig, S., Courchet, J., Lewis, T. L., Jr, Losón, O. C., Hellberg, K., Young, N. P., Chen, H., Polleux, F., Chan, D. C., & Shaw, R. J., (2016), "Metabolism. AMP-activated protein kinase mediates mitochondrial fission in response to energy stress" Science (New York, N.Y.), 351(6270), 275–281.

[42] Dasgupta, B., & Milbrandt, J., (2009), "AMP-activated protein kinase phosphorylates retinoblastoma protein to control mammalian brain development", Developmental cell, 16(2), 256–270.

[43] Zadra, G., Batista, J. L., & Loda, M., (2015), "Dissecting the Dual Role of AMPK in Cancer: From Experimental to Human Studies", Molecular cancer research: MCR, 13(7), 1059–1072.

[44] Myers, R. W., Guan, H. P., Ehrhart, J., Petrov, A., Prahalada, S., Tozzo, E., Yang, X., Kurtz, M. M., Trujillo, M., Gonzalez Trotter, D., Feng, D., Xu, S., Eiermann, G., Holahan, M. A., Rubins, D., Conarello, S., Niu, X., Souza, S. C., Miller, C., Liu, J., Sebhat, I. K., (2017), "Systemic pan-AMPK activator MK-8722 improves glucose homeostasis but induces cardiac hypertrophy", Science (New York, N.Y.), 357(6350), 507–511.

[45] Hanahan, D., & Weinberg, R. A., (2011), "Hallmarks of cancer: the next generation", Cell, 144(5), 646–674.

[46] Degterev, A., & Yuan, J., (2008), "Expansion and evolution of cell death programmes", Nature reviews. Molecular cell biology, 9(5), 378–390.

[47] White E., (2012), "Deconvoluting the context-dependent role for autophagy in cancer", Nature reviews. Cancer, 12(6), 401–410.

[48] Ma, J., Xue, H., He, L. H., Wang, L. Y., Wang, X. J., Li, X., & Zhang, L., (2021), "The Role and Mechanism of Autophagy in Pancreatic Cancer: An Update Review", Cancer management and research, 13, 8231–8240.

[49] Muñoz-Pinedo C., (2012), "Signaling pathways that regulate life and cell death: evolution of apoptosis in the context of self-defense", Advances in experimental medicine and biology, 738, 124–143.

[50] Galluzzi, L., Kepp, O., Chan, F. K., & Kroemer, G., (2017), "Necroptosis: Mechanisms and Relevance to Disease", Annual review of pathology, 12, 103–130.

[51] Chen, X., Zeh, H. J., Kang, R., Kroemer, G., & Tang, D., (2021), "Cell death in pancreatic cancer: from pathogenesis to therapy", Nature reviews. Gastroenterology & hepatology, 18(11), 804–823.

[52] Szeremeta, D., Knaś, M., Długosz, E., Krzykała, K., Mrozek-Wilczkiewicz, A., Musioł, R., & Móricz, Á. M., (2018), "Investigation of antibacterial and cytotoxic potential of phenolics derived from *Cistus incanus* L. by means of thin-layer chromatography-direct bioautography and cytotoxicity assay", 41, 349-357.

[53] Web 2, (2023), http://biodiversitycyprus.blogspot.com/2016/03/cistus-creticus-l-cyprus.html, (Accessed on 3rd July 2023).

[54] Papaefthimiou, D., Papanikolaou, A., Falara, V., Givanoudi, S., Kostas, S., & Kanellis, A. K., (2014), "Genus Cistus: a model for exploring labdane-type diterpenes' biosynthesis and a natural source of high value products with biological, aromatic, and pharmacological properties", Frontiers in chemistry, 2, 35.

[55] Stępień A, Aebisher D, Bartusik-Aebisher D., (2018), "Biological properties of *Cistus* species", Journal of Clinical and Experimental Medicine, 16(2) 127-132.

[56] Lardos, A., Prieto-Garcia, J., & Heinrich, M., (2011), "Resins and Gums in Historical Iatrosophia Texts from Cyprus - A Botanical and Medico-pharmacological Approach", Frontiers in pharmacology, 2, 32.

[57] Skorić, M., Todorović, S., Gligorijević, N., Janković, R., Živković, S., Ristić, M., & Radulović, S., (2012), "Cytotoxic activity of ethanol extracts of in vitro grown *Cistus creticus* subsp. creticus L. on human cancer cell lines", Industrial Crops and Products, 38, 153–159.

[58] Dimas, K., Papadaki, M., Tsimplouli, C., Hatziantoniou, S., Alevizopoulos, K., Pantazis, P., & Demetzos, C., (2006), "Labd-14-ene-8,13-diol (sclareol) induces cell cycle arrest and apoptosis in human breast cancer cells and enhances the activity of anticancer drugs", Biomedicine & pharmacotherapy, 60(3), 127–133.

[59] Cicenas, J., Kvederaviciute, K., Meskinyte, I., Meskinyte-Kausiliene, E., Skeberdyte, A., & Cicenas, J., (2017)., "KRAS, TP53, CDKN2A, SMAD4, BRCA1, and BRCA2 Mutations in Pancreatic Cancer. Cancers", 9(5), 42.

[60] Greenwell, M., & Rahman, P. K., (2015), "Medicinal Plants: Their Use in Anticancer Treatment", International journal of pharmaceutical sciences and research, 6(10), 4103–4112.

[61] Mahajan, S., & Tuteja, N., (2005), "Cold, salinity and drought stresses: an overview", Archives of biochemistry and biophysics, 444(2), 139–158.

[62] Berridge, M. V., Herst, P. M., & Tan, A. S., (2005), "Tetrazolium dyes as tools in cell biology: new insights into their cellular reduction", Biotechnology annual review, 11, 127–152.

[63] Wang, X., Li, W., Jiang, H., Ma, C., Huang, M., Wei, X., Wang, W., & Jing, L., (2022), "Zebrafish Xenograft Model for Studying Pancreatic Cancer-Instructed Innate Immune Microenvironment", International journal of molecular sciences, 23(12), 6442.

[64] Liu, Z., Ren, Z., Zhang, J., Chuang, C. C., Kandaswamy, E., Zhou, T., & Zuo, L., (2018), "Role of ROS and Nutritional Antioxidants in Human Diseases", Frontiers in physiology, 9, 477.

[65] Nakamura, H., & Takada, K., (2021), "Reactive oxygen species in cancer: Current findings and future directions", Cancer science, 112(10), 3945–3952.

[66] Kamihara, Y., Takada, K., Sato, T., Kawano, Y., Murase, K., Arihara, Y., Kikuchi, S., Hayasaka, N., Usami, M., Iyama, S., Miyanishi, K., Sato, Y., Kobune, M., & Kato, J. (2016), "The iron chelator deferasirox induces apoptosis by targeting oncogenic Pyk2/β-catenin signaling in human multiple myeloma", Oncotarget, 7(39), 64330–64341.

[67] Boren, J., & Brindle, K. M., (2012), "Apoptosis-induced mitochondrial dysfunction causes cytoplasmic lipid droplet formation", Cell death and differentiation, 19(9), 1561–1570.

[68] Chazotte B., (2011), "Labeling nuclear DNA using DAPI", Cold Spring Harbor protocols, 2011(1), 5556.

[69] Yin, X., Xu, R., Song, J., Ruze, R., Chen, Y., Wang, C., & Xu, Q., (2022), "Lipid metabolism in pancreatic cancer: emerging roles and potential targets", Cancer communications (London, England), 42(12), 1234–1256.

[70] Mescam, M., Vinnakota, K. C., & Beard, D. A., (2011), "Identification of the catalytic mechanism and estimation of kinetic parameters for fumarase", The Journal of biological chemistry, 286(24), 21100–21109.

[71] Lama-Sherpa, T. D., Jeong, M. H., & Jewell, J. L., (2023), "Regulation of mTORC1 by the Rag GTPases", Biochemical Society transactions, 51(2), 655–664.

[72] Kimura, T., Hayama, Y., Okuzaki, D., Nada, S., & Okada, M., (2022), “The Ragulator complex serves as a substrate-specific mTORC1 scaffold in regulating the nuclear translocation of transcription factor EB”, The Journal of biological chemistry, 298(3), 101744.

BIOGRAPHY

Burçin Özbekle graduated from her Bachelor of Science program in Genetic and Bioengineering Department at Yeditepe University in 2020. During her BSc, she completed her internship in Environmental Biotechnology Institute at Istanbul Technical University. She has started her Master of Science program in Institute of Biotechnology at Gebze Technical University in 2021. During her MSc. Program, she worked in TUBITAK 1001 (Project no: 118Z100) and TUBITAK 1002 (Project no: 122Z186) projects as a research scholar. In business life, she worked as a clinical research project coordinator in the oncology field.

APPENDICES

Appendix A: Publications Within the Scope of Thesis Study

Ozbekle B, Arisan E.D., (2022), "Investigation of Anti-cancer Effects of *Cistus creticus* L. Grown Under Salinity Stress in Pancreatic Cancer Cell Lines" 4th Congress of Cell Death Research Society-Turkey with International Participation, Turkey, 17-19 March 2022 (Poster Presentation First Prize).